



Department of Chemistry and Biochemistry

900 Yukon Dr., Reichardt Building Room 194
P.O. Box 756160
Fairbanks, AK 99775-6160
(907) 474-5510 • Fax (907) 474-5640
chemistry.uaf@alaska.edu • www.uaf.edu/chem

America's Arctic University

29 December 2014
wrsimpson@alaska.edu

To: ACP (Editor Steve Brown)

We have replied to all referee questions via the online discussion forum. These comments include discussion of the sections of text that were modified. For convenience, we include both replies to the referees (downloaded from ACPD) in addition to a latex-diff version of the manuscript showing the changes we made in this response PDF file. We hope that this documentation addresses the referees concerns and that the manuscript is now acceptable for publication.

Interactive comment on “Meteorological controls on the vertical distribution of bromine monoxide in the lower troposphere” by P. K. Peterson et al.

P. K. Peterson et al.

wrsimpson@alaska.edu

Received and published: 27 December 2014

We thank Anonymous Referee #1 for the constructive comments on this manuscript. In our response, we first address the overarching concerns of the reviewer, followed by addressing individual comments. We denote points that that the reviewer raises using bold text followed by our reply. Please also see our replies to Anonymous Referee #2.

Main concerns. 1) MAX-DOAS analysis shown in this study is a two-step approach, where an “ad-hoc” optimal estimation (EO) is used to first retrieve the aerosol extinction coefficient profile and second - BrO profile. The 2nd step depends on the 1st step. Since the authors rightfully criticize applicability of the OE to the 2nd step where DOF is approximately 2 and full profile cannot be

C10528

reliably retrieved, the same argument applies to the 1st step (same MAX-DOAS data are used). The authors have to demonstrate that the OE in the first step provide reliable enough profiles for the 2nd step and that the error from the aerosol extinction profile retrieval does not introduce a significant error in LT-VCD BrO analysis. In addition, the retrieved aerosol extinction profile is MAX-DOAS averaging kernel smoothed profile with low sensitivity above 1 km. The forward RT modeling in the second step requires the “true” profile. It will be interesting to see what effect this resolution degradation has on the LT-VCD BrO analysis.

Rather than criticizing the applicability of optimal estimation (OE) in this case, we merely seek to clarify the limitations of profiles retrieved in this manner, as they lend themselves to overinterpretation. The use of a retrieved aerosol particle extinction profile, rather than the true profile, will introduce errors in the resulting BrO profile and these errors should be quantified. One can estimate the errors in BrO retrieval due to uncertainties in the aerosol particle extinction profile by examining the sensitivity of the BrO retrieval to perturbations in the aerosol particle extinction profile. We retrieved BrO profiles from the same BrO dSCD data over an ensemble of varying aerosol particle extinction profiles, and examined the resulting variability in the quantities discussed in this manuscript. We found that the LT-VCD was not heavily influenced by changes in the aerosol profile, with an estimated error of 4.6% (1 Sigma), which is lower than error introduced by uncertainties in the BrO dSCD measurements. The ratio's retrieved $VCD_{200m}/LT - VCD$ have an estimated error of 4.9% (1 Sigma). Thus, it is reasonable to conclude that our conclusions about the vertical structure of halogen events at Barrow presented in this manuscript are not substantially influenced by errors in aerosol retrieval. We have added a summary of this analysis to the revised manuscript at the end of Section 2.4.

C10529

2) Since BrO activation is linked to heterogeneous reactions any dependence on other physical parameters (e.g. temperature) should be done for the same aerosol conditions. Under strong wind conditions it is also important to know the source of air masses brought into the MAX-DOAS instrument field of view. Are there any independent aerosol measurements at the NOAA and/or ARM Barrow facilities that can give information about the dependence of wind speed and aerosols? In general, Arctic climatology is very complicated and decoupling of different meteorological parameters is not straightforward. Please also include information whether there were passing polar lows and/or cyclones.

We agree that decoupling of differing parameters is not straightforward. We examined variations of BrO with temperature and wind speed under similar aerosol loadings and did not find anything that would change or add to the presented analysis. We include Fig. 1 of this response that shows some further analysis. That figure shows the response of BrO to various environmental parameters at various extinction levels is shown in two scatter plots. On the left, the response of BrO to temperature changes in various bins of aerosol particle extinction is shown. These data are split into three bins, low extinction shown in blue x's, moderate extinction, shown in red circles, and high extinction, shown in green diamonds. The right plot is identically structured, showing the relationship between BrO and wind speed. We also examined air mass history, and found that for this field campaign, measured air masses had similar origins and contact with sea ice areas, making it difficult to discuss the influence of air mass history on observed BrO. Please see our response to Reviewer 2, as well as Section 3.3 of the revised manuscript for an expanded discussion of our air mass history analysis. There were some stormy events over the measurement period, but measurements during these periods constitute a small part of the data set. We examined the relationship between BrO and air pressure, but did not find anything that would substantially add to the manuscript.

C10530

p. 23954 , I 24. The sensitivity to upper troposphere and lower stratosphere is reduced but still present especially at SZA > 75deg. How do the authors account for it in the analysis at SZA > 75deg?

In our spectral fitting, a near temporally coincident zenith spectrum is used as the reference, which (as the referee notes) removes most of the influence from higher altitudes. In principle, one could use a fixed reference spectrum (e.g. at local solar noon on a clear day) for the fitting, but that choice makes the analysis more dependent on long-term drifts, so we instead take the "local zenith" reference choice. Due to this choice, there is a small influence at SZA > 75 degrees, but for consistency, we do not treat data collected at SZA > 75 degrees differently from other data. To reduce influence from the spectra even closer to twilight, we do not analyze data collected at SZA > 85 degrees. Overall, data collected between 75 and 85 degrees SZA represents only 30% of our data, so the inclusion or exclusion of these data would not change the findings of the manuscript.

p. 23954 Methods, MAX-DOAS measurements: I suggest that all the data presented in this work (IL1, BARC, SIMS, sondes) are described in this section, including description of the measurement locations and azimuthal direction of MAX-DOAS measurements. It will also be helpful to get an idea about the meteorological conditions during the campaign and description of the air masses that are traversed by the measured photons. How do you treat cloudy data?

We have modified the methods section to include all requested information, and added information on the azimuth of the DOAS, as well as modifying Fig. 5 to better show the environmental conditions around the measurement sites, as well as the azimuths of each DOAS instrument. Please see Section 2.5, last paragraph of the revised manuscript. We do not screen for cloudy data other than using the degrees of freedom

C10531

based filtering described in section 2.4. Due to the relationship between AOD and aloft DOF shown in the left panel of Fig. 3, it is likely any data with low clouds are excluded as a result of the DOF filtering.

p. 23955, I. 4 How well is the optical bench temperature maintained? Ocean Optics spectrometers tend to have strong temperature dependence of the slit function (resolution).

The standard deviation of the spectrometer temperature is 0.6 degrees. We have included this information in the revised manuscript.

p. 23955, I. 15. Add “transfer” after instrumental

We have made this change.

p. 23955, I. 20 It will be more meaningful to present residual OD RMS as a function of viewing elevation angle. Since DOAS fitting errors are linearly related to the residual OD RMS I suggest including BrO/O4 DOAS fitting errors as a function of elevation angle too.

Please see Table 1 of this response for this information. This table has been included in the supplemental material.

p. 23956, I. 13. What is the a priori covariance matrix? What are the assumptions about the aerosol optical properties? Are you applying any correction factors to the measured dSCD(O4)? Could you estimate BrO 200m-VCD and LT-VCD errors due to aerosol profile error?

C10532

The aerosol assumptions are detailed in Frieß et al. (2011).

“Since the radiative transfer near the surface is frequently affected by blowing snow, the aerosol optical properties are set to values typical for clean ice crystals, with a single scattering albedo of 0.999982 and a Henyey Greenstein phase function with an asymmetry parameter of $g = 0.89$ [Dominé et al., 2008, and references therein]. The aerosol extinction profile is retrieved in the lowermost 2 km of the atmosphere on a 100 m vertical grid... In each iteration, the a priori error, i.e., the square root of the diagonal elements of the a priori covariance matrix, is set to three times the a priori extinction, while the non-diagonal elements of S_a are set to zero.”

We have added a reference to this information in the revised manuscript, page 8, lines 1-3. We have also added detail on the a priori covariance matrix on page 8, lines 8-10 of the revised manuscript. Please see our response to the reviewer’s first point for estimations of the error associated with these quantities.

p. 23957, I. 25 How do you define “the layer in which the observer resides” from a MAX-DOAS perspective?

In the case of this study we mean the lowest portion of the boundary layer when the measured photons traverse a path tangent to the ground. We have clarified this point in the text. Please see page 9, lines 18-20 of the revised manuscript.

p. 23959, I. 19, Payne et al (2009) does not “describe how to calculate the BrO averaging kernel for the coarsened grid” the paper applies the method to methane not BrO. Please check your reference or rephrase the sentence. The cutoff 0.7 was used for satellite nadir measurements of methane. While it is likely it is applicable to MAX- DOAS ground-based measurements I would suggest doing some sensitivity studies to confirm this. Payne, V. H., Clough,

C10533

S. A., Shephard, M. W., Nassar, R., and Logan, J. A.: Information centered representation of retrievals with limited degrees of freedom for signal: application to methane from the tropospheric emission spectrometer, *J. Geophys. Res.*, 114, D10307, doi:10.1029/2008JD010155, 2009. 23953, 23959

We agree with the reviewer that this wording should be changed. Please see page 11, lines 13-15 of the revised manuscript. Payne et al detail a general method for reducing profiles retrieved via optimal estimation. They then use methane retrievals as an example for the application of this general technique. The application of this technique to BrO is not mentioned in the Payne et al work. We agree that the 0.7 is somewhat arbitrary, we explored multiple values, and found that the conclusions did not change as long as the cutoff was above 0.4, thus we chose to remain consistent with previous work.

p. 23962, I.15 Please replace “observes” for “retrieves”. Technically O3 absorption is present in MAX-DOAS data.

We have made this change. We also do fit for O₃, we just do not interpret the retrieved dSCD values because of the complexity of the radiative transfer of ozone and the temperature dependence of the cross section.

p. 23963, I. 25 What do you mean by "large changes in the environment in MAX-DOAS field of view"? Are there any significant differences in elevation, snow cover, landscape, and aerosol types? If there is a significant difference along the line of sight how did you treat it in RT modeling? Please show MAX-DOAS azimuthal direction on Figure 5.

C10534

As shown in the revised Fig. 5, the instrument at the BARC building overlooks a large lead which has a convective plume along the line of sight. Since both radiative transfer models are 1D, only changes in the vertical direction are modeled. Thus any reduction in pathlength due to a lead cloud would be modeled as a path-averaged increase in near surface extinction rather than an obstruction in the view direction. This is a potential source of error in the aerosol profile, and resulting BrO profile. We discuss this in Section 3.4 of the revised manuscript. Please see page 17, lines 6-8.

p. 23964, I. 4 Figure 6 gives an impression that a significant number of time coincident observations exist. After closer inspection CIMS data are mainly shown for nighttime when MAX-DOAS instrument did not measure. Why there are so many "holes" in CIMS data?

This CIMS instrument was also used to conduct snow chamber experiments during BROMEX, creating gaps in the time series of ambient BrO. We have pointed this out in the revised manuscript, page 16, lines 18-20.

p. 23964, I. 6 Could you please elaborate why do you claim that the differences in observations at IL1 and BARC explain differences between BARC and CIMS locations. What is the azimuth angle of BARC and IL1 MAX-DOAS observations? Where they pointing towards each other? What were the meteorological conditions at the 3 sites?

Meteorological conditions were similar at the three sites throughout the inter-comparison. The azimuth of the DOAS at BARC was 27 degrees east of north, while the azimuth of IL1 was 2 degrees east of north. These azimuths are similar enough that we are confident that any differences do not arise from viewing geometry

C10535

differences. However, as show in the revised Fig. 5 of the manuscript, the instrument at BARC overlooks a recurring lead, while the instrument at IL1 does not. Please see our response to Reviewer 2, point number 2, as well as page 17, lines 6-8 of the revised manuscript for additional discussion of this feature.

p. 23965, I. 10 You compare daily averaged MAX-DOAS data with the 15:30 AKSD sonde data. Were the meteorological conditions constant during any particular day? Would the conclusion change if comparison done using time coincident or +/- 1 hr data?

While the meteorological conditions are not constant throughout the day, we feel the comparison of daily averaged LT-VCDs with daily soundings still provides insight into the role of atmospheric stability. We found that the use of temporally coincident data or data off an hour either way did not alter the conclusions.

p. 23965, I. 19. Could you please explain what you mean by “The short diurnal time scales of the temperature gradient.”

We simply mean to point out that the temperature gradient likely varies with a higher frequency than can be observed with twice daily sounding data. We have clarified this point. Please see Page 18. lines 7-10, of the revised manuscript for the modified text.

p. 23965, Since halogen activation is related to heterogeneous reactions it might give more insight if any dependence on temperature is derived from the data bins collected under the same aerosol loading conditions. Since LT-VCD accuracy has a stronger dependence on the aerosol loading than 200m VCD I suggest also including data where only 200m VCD is shown.

C10536

While we agree that this is a useful analysis, after performing said analysis, shown in Fig. 1 of this response, we did not find differing behaviour under various aerosol conditions.

p. 23967, I. 29. What is the typical PBL height during the measurement period at this location?

During OASIS, which was conducted at Barrow in 2009 during a similar time frame, PBL heights ranged from less than 100m to over 500m (Boylan et al., 2014).

I am not sure what the authors want to convey by “Therefore, the diurnal pattern of the vertical profile of BrO appears to reflect boundary layer dynamics. The observation of Pöhler et al. (2010) of decreasing surface BrO mixing ratio at higher temperatures could therefore reflect increased vertical mixing of surface sourced BrO that dilutes the surface concentration upon warming rather than being indicative of decreased halogen activation chemistry at higher temperatures.” If the source of BrO is located at the ground and shallow PBL is present (< 1000m, probably 400-600 m) convective mixing to the upper layers should not result in in- crease in measured LT-VCD (0 – 2000m). This implies that there is another source of BrO at altitudes > 200 m that is coincident with the potential PBL diurnal evolution. Do you have an independent PBL height estimation to confirm your statement about PBL diurnal evolution? It might be helpful to separate data into “colder” and “warmer” periods to see if the trend persists.

We discuss these issues in detail in our response to Reviewer 2. To address concerns raised by both reviewers, we have expanded our discussion of these observations.

C10537

Please see our response to points 4-6 raised by the second reviewer, as well as the last paragraph of section 4.1, which we have substantially revised in response to comments from both reviewers. Regarding the diurnal evolution of the PBL, this is commonly observed in Barrow, although it is less pronounced during periods of heavy inversion (Boylan et al., 2014). We have pointed this out in the revised manuscript.

Role of wind speed (4.2) and Relationship between activation and aerosol particles (4.3) might not be reliably established from LT-VCD or VCD200m/LT-VCD since LT- VCD retrieval is potentially effected by the aerosol retrieval in the 1st step and due to decreased sensitivity of MAX-DOAS at higher AOT.

The reviewer points out the limitations of our data set, which we discuss in section 4.3, page 22, lines 20-24. While the limitations of our data collection at higher AOT complicate interpretation of the role of aerosols and wind speed, Fig. 13 also shows the relationship between BrO and aerosol particle extinction in the near surface layer, where we have the greatest sensitivity. The left panel clearly shows aerosol particle extinction does not depend on wind speed, while there is an increase in BrO with increased aerosol particle extinction, which we pointed out in section 4.3. The conclusions in this paper about the role of blowing snow events and wind speed in general are clearly supported by the near-surface BrO data, in addition to the LT-VCD data. Thus, this data set reliably establishes the role of wind speed and aerosol particles during this field study. We have restructured the discussion of Fig. 13 in Section 4.3 to convey these points more clearly and address the concerns raised by the reviewer.

Figure 5. Please indicate MAX-DOAS azimuthal orientation. In addition, information about snow/ice cover will be valuable

We have modified Fig. 5 to include the requested information.

C10538

Figure 7. Please show error bars for both MAX-DOAS and CIMS data

We have modified Fig. 7 to include the requested information.

References

- Boylan, P., Helmig, D., Staebler, R., Turnipseed, A., Fairall, C., and Neff, W.: Boundary layer dynamics during the Ocean-Atmosphere-Sea-Ice-Snow (OASIS) 2009 experiment at Barrow, AK, *Journal of Geophysical Research: Atmospheres*, 119, 2261–2278, 10.1002/2013JD020299, <http://doi.wiley.com/10.1002/2013JD020299>, 2014.
- Frieß U., Sihler, H., Sander, R., Pöhler, D., Yilmaz, S., and Platt, U.: The vertical distribution of BrO and aerosols in the Arctic: Measurements by active and passive differential optical absorption spectroscopy, *Journal of Geophysical Research*, 116, 10.1029/2011JD015938, <http://www.agu.org/pubs/crossref/2011/2011JD015938.shtml>, 2011.

C10539

Table 1. Errors for MAX-DOAS fitting over all elevation angles.

Elevation Angle	Mean RMS	Mean BrO dSCD Error	Mean O ₄ dSCD Error
1 Degree	4.1×10^{-4}	2.0×10^{13} molecules cm ⁻²	5.4×10^{41} molecules ² cm ⁻⁵
2 Degree	4.0×10^{-4}	1.9×10^{13} molecules cm ⁻²	5.3×10^{41} molecules ² cm ⁻⁵
5 Degree	3.9×10^{-4}	1.9×10^{13} molecules cm ⁻²	5.2×10^{41} molecules ² cm ⁻⁵
10 Degree	3.8×10^{-4}	1.8×10^{13} molecules cm ⁻²	5.0×10^{41} molecules ² cm ⁻⁵
20 Degree	3.6×10^{-4}	1.7×10^{13} molecules cm ⁻²	4.7×10^{41} molecules ² cm ⁻⁵

Interactive comment on Atmos. Chem. Phys. Discuss., 14, 23949, 2014.

C10540

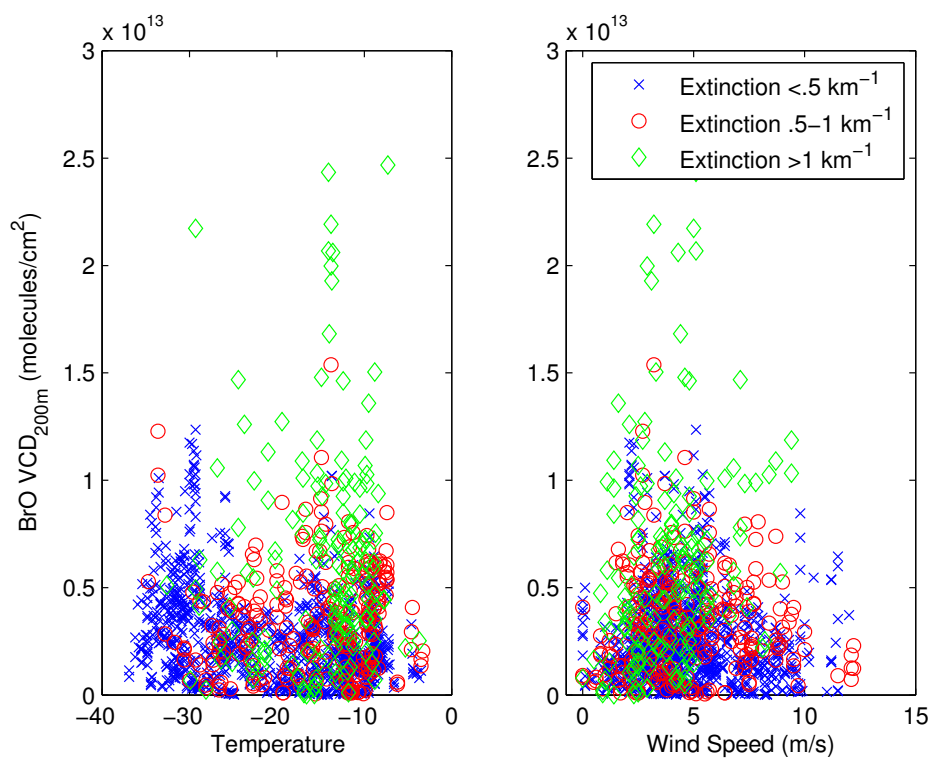


Fig. 1. Response of BrO to environmental parameters

C10541

Interactive comment on “Meteorological controls on the vertical distribution of bromine monoxide in the lower troposphere” by P. K. Peterson et al.

P. K. Peterson et al.

wrsimpson@alaska.edu

Received and published: 27 December 2014

We thank Anonymous Referee #2 for the constructive comments on this manuscript. In our response, we denote points that the reviewer raises using bold text followed by our reply. Please also see our replies to Anonymous Referee #1.

1. The paper focuses on two possible meteorological controls for BrO vertical distributions: wind speed and temperature. Analysis of temperature (stability) and wind speed is not sufficient considering the particularities of the Barrow research site where air that arrives can be influenced different histories (originated from snow, ice, the city of Barrow, etc). As pointed out by the first

C10542

reviewer, the issues of airmass origin must also be considered in this analysis. For example, what is the influence of wind direction on BrO VCD,200m and BrO VCD,LT?

The reviewer points out that our analysis does not address air mass history, which has also been shown to influence BrO. Over the course of these measurements, all measured airmasses spent at least 25% of the past 72 hours in contact with sea ice while 90% of measured air masses spent over 75% of the past 72 hours over sea ice. While there is an influence of airmass history on the levels of BrO, given the high levels of sea ice contact observed throughout the campaign, it is unlikely that the variability of BrO observed during this campaign can be attributed to variations in air mass history. This is not to say that air mass history does not play a role, we simply point out that this data set is unsuitable for discerning that role. We are currently working on a separate manuscript that draws on observations from multiple years to look at the influence of air mass history on BrO observations at coastal sites. See Fig. 1 of this reply that shows statistics on the history of observed air masses. The left panel shows contact with sea ice areas in the previous 72 hours, calculated using methods detailed in (Simpson et al., 2007). The right panel shows the wind directions observed during the campaign. We have also added Section 3.3 to the revised manuscript to address these concerns.

2. It is concerning that in Figure 6 all of the area in gray is excluded from the correlation presented in Figure 7. Is there a known reason for the horizontal gradient in BrO during this period? A more in depth analysis (including airmass history) may provide insight onto these differences, which should be discussed in the paper.

This time period coincides with a convective plume from an open lead north of the

C10543

BARC building that is visible on MODIS imagery. Because DOAS is a path-averaged measurement, it is possible that this convective lead plume would cause horizontal gradients in BrO. As this mechanism is purely speculative at this point, we felt it best just to show the existence of a horizontal gradient. We have modified Fig. 5 to show the existence of the lead in the DOAS view direction and added a discussion of the lead opening to Section 3.4. Please see page 17, lines 6-8 of the revised manuscript.

3. Figures 10 and 11 show the BrO VCD 200m as a function of temperature (Figure 10) and wind speed (Figure 11). However, other controlling factors (e.g. available sunlight and ozone mixing ratios) have not been considered as possible driving factors controlling BrO VCD,200m and VCD,LT. Although the influence of ozone has somewhat been taken into account by excluding very low ozone airmasses, it does not seem a fair comparison to consider all measurements together, without considering also cloud cover and/or time of day in order to consider the amount of available sunlight in these correlations.

We agree that simple univariate analysis is insufficient to fully elucidate the impacts of temperature and wind speed on BrO, however this data set is not large enough to provide an adequate sample size across the range of cloud conditions and daylight conditions proposed by the reviewer. Additionally, cloudy conditions make the use of MAX-DOAS to measure BrO problematic, given the relationship between AOD and the information content of the aloft layer.

4. In Figure 12, the authors show that BrO in the lowest 200m peaks at the beginning and end of the day. What does it mean that BrO peaks when there is no longer enough available sunlight to make MAX-DOAS measurements? Does it mean, that there is still enough available sunlight to drive Br₂ ↔ BrO photochemistry, but not enough to measure? Is this a real feature?

C10544

Given the relationship between atmospheric stability and LT-VCD discussed in this paper, we find it reasonable that the diurnal profile of the VCD_{200m} is consistent with a surface source of BrO being diluted throughout an expanded boundary layer at midday. However, as discussed below, the growth of the LT-VCD is not consistent with purely dilution. Please see Section 4.1 of the revised manuscript for a discussion of this feature.

5. It is interesting that the VCD,LT-VCD peaks at a different time of day than the BrO VCD,200m. This may have to do with the combination of available sunlight and mixing processes. Has the balloon sounding data been used to look at the temperature profiles above 200 m in order to investigate the amount of vertical transport occurring at mid-day? Is the peak in the lowest 2 km from a surface source of reactive bromine, or is it from bromine already in the free troposphere? Airmass histories (FLEXPART or HYSPLIT) and additional balloon sounding data are needed to suggest the origins of the measured BrO within the VCD,LT.

Interestingly, the growth of the LT-VCD is not consistent with dilution, but indicates an increase in activation of bromine at midday, this could be due to increased sunlight around local solar noon, activation occurring aloft, or an increased BrO lifetime aloft. We find it unlikely that this systematic peak at a particular time of day would indicate increased transport of free-tropospheric BrO to the measurement site as there is currently no physical mechanism to explain that. Additionally, given the poor resolution and lack of sensitivity of MAX-DOAS at higher altitudes, we do not feel these data allow us to unambiguously differentiate between boundary layer BrO and free tropospheric BrO. Thus, we do not feel it is appropriate to discuss the existence, or lack thereof, of free tropospheric BrO at the measurement site. We have added a discussion of possible explanations for this behavior to the discussion, last paragraph of section 4.1

C10545

of the revised manuscript.

6. These type of diurnal profiles in BrO (peak in the morning and afternoon) along with a dip at mid-day have been observed already at Summit (See Figure 6 of Stutz et al., 2011). This was used in part to suggest a small snow source of reactive bromine even far from the coast. The authors should discuss if the same type of diurnal profile in their VCD,200m (albeit at a different site and time of year) is similar evidence for a snow source of bromine.

We agree that our findings constitute similar evidence for snow-sourced bromine. We have included a discussion of this work in the discussion section, page 20, lines 24-26 of the revised manuscript.

7. The conclusions section of the paper should be expanded to include a better perspective on what this paper adds to our understanding of bromine sources and chemistry. In comparison to the paper, the conclusion is much too brief and should include a better synthesis of the science results and their context.

We have expanded the conclusions to address these concerns. Please see page 25, lines 1-9, of the revised manuscript for additions to the conclusions.

8. The title of the paper should be changed to "Temperature and wind speed controls" unless further analysis of the meteorology during the campaign is presented in the paper.

The proposed change misrepresents the information contained in the paper, as

C10546

many conclusions of the paper are based on atmospheric stability, which would not be implied by the proposed revised title. While we do not address every aspect of meteorology, this work is a substantial analysis of the response of BrO to various meteorological factors.

9. The statements about using bromine source parameterizations based on wind speed in 3D models are currently not totally supported by the data presented in the paper. Specifically - I object to the text which states, "BrO may show an apparent relationship to wind speed" on Page 23969. The authors have not done enough analysis to determine how bromine gets out of the boundary layer into the free troposphere, where it is likely to be detectable by satellites, which may very well correlated with wind speed. The authors should be more careful in their wording, because this may not be just an apparent, but an actual correlation of BrO in the free troposphere with surface wind speeds. Although, wind speed may not represent the first step in the bromine release process.

Our objective in the second paragraph of section 4.2 was to convey two points.

1. That our data do not support an increase in activation of BrO at high wind speeds.
2. That the discrepancies in the conclusions of our study vs previous work relying on satellite measurements may be due to differing viewing geometry.

We agree that our wording should be improved and have modified the text to convey these points more clearly. Please see modified text at the end of Section 4.2 of the revised manuscript.

C10547

References

Simpson, W. R., Carlson, D., Hönninger, G., Douglas, T. A., Sturm, M., Perovich, D., and Platt, U.: First-year sea-ice contact predicts bromine monoxide (BrO) levels at Barrow, Alaska better than potential frost flower contact, *Atmospheric Chemistry and Physics*, 7, 621–627, 10.5194/acp-7-621-2007, <http://www.atmos-chem-phys.net/7/621/2007/>, 2007.

Interactive comment on *Atmos. Chem. Phys. Discuss.*, 14, 23949, 2014.

C10548

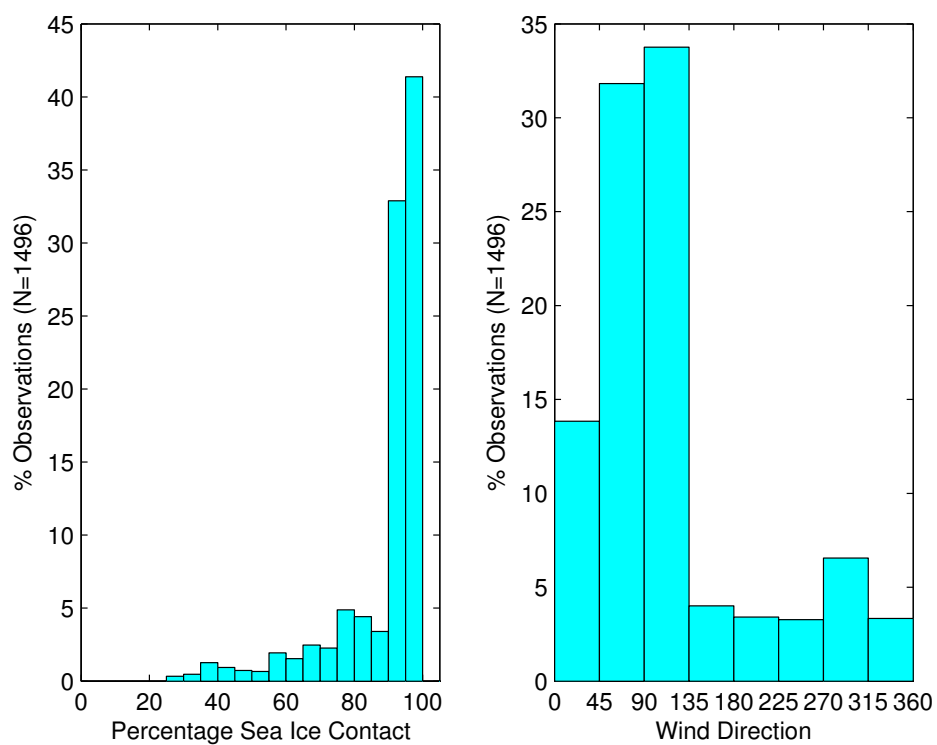


Fig. 1. Sea ice contact and local wind direction of sampled air masses

C10549

Meteorological controls on the vertical distribution of bromine monoxide in the lower troposphere

P. K. Peterson¹, W. R. Simpson¹, K. A. Pratt^{2,*}, P. B. Shepson^{2,3}, U. Frieß⁴, J. Zielcke⁴, U. Platt⁴, S. J. Walsh¹, and S. V. Nghiem⁵

¹Department of Chemistry and Biochemistry, Geophysical Institute, University of Alaska Fairbanks, Fairbanks, Alaska, USA

²Department of Chemistry, Purdue University, West Lafayette, Indiana, USA

³Department of Earth, Atmospheric and Planetary Sciences, Purdue University, West Lafayette, Indiana, USA

⁴Institute for Environmental Physics, University of Heidelberg, Germany

⁵Jet Propulsion Laboratory, California Institute of Technology, Pasadena, California, USA

*now at: Department of Chemistry and Department of Earth & Environmental Sciences, University of Michigan, Ann Arbor, Michigan, USA

Correspondence to: W. R. Simpson (wrsimpson@alaska.edu)

Abstract

Multiple axis differential absorption spectroscopy (MAX-DOAS) measurements of bromine monoxide (BrO) probed the vertical structure of halogen activation events during March–May 2012 at Barrow, Alaska. An analysis of the BrO averaging kernels and degrees of freedom obtained by optimal-estimation-based inversions from raw MAX-DOAS measurements reveals the information is best represented by reducing the retrieved BrO profile to two quantities, the integrated column from the surface through 200 m ($VCD_{200\text{ m}}$), and the lower tropospheric vertical column density (LT-VCD), which represents the integrated column of BrO from the surface through 2 km. The percentage of lower-tropospheric BrO in the lowest 200 m was found to be highly variable ranging from shallow layer events, where BrO is present primarily in the lowest 200 m to distributed column events where BrO is observed at higher altitudes. The highest observed LT-VCD events occurred when BrO was distributed throughout the lower troposphere, rather than concentrated near the surface. Atmospheric stability in the lowest 200 m influenced the percentage of LT-VCD that is in the lowest 200 m, with inverted temperature structures having a first-to-third quartile range (Q1–Q3) of $VCD_{200\text{ m}}/LT\text{-VCD}$ from 15–39 % while near neutral temperature structures had a Q1–Q3 range of 7–13 %. Data from this campaign show no clear influence of wind speed on either lower-tropospheric bromine activation (LT-VCD) or the vertical distribution of BrO, while examination of seasonal trends and the temperature dependence of the vertical distribution supported the conclusion that the atmospheric stability affects the vertical distribution of BrO.

1 Introduction

The seasonal return of sunlight during late winter in the polar regions is associated with production of reactive halogens (e.g. Br, BrO, Cl) from saline ice surfaces (Abbatt et al., 2012; Saiz-Lopez and von Glasow, 2012). These halogen species influence boundary layer chemistry through phenomena such as boundary layer ozone depletion events (ODEs) (Barrie

et al., 1988; Simpson et al., 2007b) and mercury deposition events (MDEs) (Schroeder et al., 1998; Steffen et al., 2008). While the production mechanism of these halogens is not fully understood, modeling (e.g. Fan and Jacob, 1992; Mozurkewich, 1995; Lehrer et al., 2004; Piot and von Glasow, 2007; Yang et al., 2010; Parrella et al., 2012; Toyota et al., 2014), laboratory (e.g. Fickert et al., 1999; Huff and Abbatt, 2000; Wren et al., 2013) and field studies (e.g. Foster et al., 2001; Spicer et al., 2002; Toom-Sauntry and Barrie, 2002; Krnavek et al., 2012; Pratt et al., 2013; Liao et al., 2014) point to heterogeneous chemistry involving salts present on ice surfaces (e.g. NaBr, NaCl) as important sources of reactive halogens.

Multiple studies have examined the vertical extent of ODEs that result from halogen chemistry and have shown ODE vertical structure to be highly variable (Bottenheim et al., 2002b; Jones et al., 2010; Helmig et al., 2012; Oltmans et al., 2012). Jones et al. (2010) suggest a link between ozone depletion at higher altitudes and low pressure systems (storms) from Antarctic observations, but also point out that this relationship may not be the case in the Arctic due to differing meteorology. Ozone sonde data from ARCTAS/ARCPAC and OASIS campaigns presented in Oltmans et al. (2012) show the vertical extent of ozone depletion varies between 200 and 1000 m, and that this difference may be tied to the origin of the observed air masses in addition to the local meteorology. Although the profile of ozone depletion gives some insights into the vertical structures of the reactive halogens that deplete ozone, the differing chemical lifetimes of ozone (a day to longer) and reactive halogens (minutes to hour unless recycled by heterogeneous chemistry on particles) may mean that halogen vertical profiles differ from ozone depletion profiles. Tackett et al. (2007) present a view from tethered balloon measurements of a stratified lower boundary layer, in which the rates of ozone and Hg depletion are determined by downward mixing into the halogen-chemistry-active surface layer. Moore et al. (2014) found that both ozone and mercury levels recovered to higher levels when vertical mixing induced by sea ice leads had recently influenced the observed airmasses, but the effect of this mixing on reactive halogens is not known. The work of Frieß et al. (2011) used MAX-DOAS observations along with optimal-estimation-based inversions to retrieve full-BrO concentration profiles and showed

significant variability in vertical structure with reactive halogens typically being in the lowest ~ 1 km of the atmosphere, similar to the ozone depleted layer.

The physical mechanisms for the transport of reactive halogens from the snow pack to the boundary layer and recycling of those halogens aloft are still poorly understood. Given the short lifetime of BrO in the absence of heterogeneous recycling (McConnell et al., 1992; Platt and Hönninger, 2003), it is likely that some sort of aerosol particles (Fan and Jacob, 1992), either from blowing snow or other sources are required to sustain halogen activation aloft. Recent literature in particular has focused on the role of blowing snow events in halogen activation (e.g. Jones et al., 2009, 2010; Yang et al., 2010; Frieß et al., 2011). In particular, Jones et al. (2009) used O₃ observations at Halley station in Antarctica, to derive a model for the dependence of ODEs on wind speed. Jones et al. (2009) suggest that there are two environmental regimes that favor local halogen activation and subsequent ozone depletion. One regime consists of low wind speeds and a stable boundary layer, the other requires high winds and the presence of blowing snow. Blowing snow events occur when high winds loft snow, potentially enhancing available snow surface area available for reaction. Blowing snow may shift reactive halogens aloft through reactions on the blowing snow or aerosol particles produced by sublimed blowing snow (Jones et al., 2009, 2010; Yang et al., 2010; Frieß et al., 2011). Comparison of satellite-observed column BrO data with modeling results by Yang et al. (2010) suggests that blowing snow events may be sufficient to explain the majority of halogen activation events observed via satellite. In contrast, Halfacre et al. (2014) conducted an analysis at a variety of locations across the Arctic and found no relationship between observed ozone and wind speed, suggesting that high wind speeds, and consequently blowing snow, may not play a major role in ozone depletion. Again, because of the differing chemical lifetimes of ozone and reactive halogens, using ozone depletion as a proxy for halogen activation requires caution.

To examine these ideas further, it is necessary to observe both the total amount of reactive halogens, and their distribution throughout the lower troposphere. While satellite measurements (e.g. Wagner and Platt, 1998; Richter et al., 1998; Chance, 1998) provide extensive spatial coverage of the Arctic, they only measure the total column of BrO, and do

not provide vertical profile or near surface information. Multiple methods exist to separate total column measurements into stratospheric and tropospheric components (e.g. Theys et al., 2011; Salawitch et al., 2010; Koo et al., 2012; Sihler et al., 2012). However, discrepancies still exist between ground based and satellite based measurements, potentially due to clouds masking portions of the tropospheric BrO column from satellite views. Additionally, Theys et al. (2009) and Salawitch et al. (2010) showed that some of the variability of total column BrO arises from stratospheric variability, thus not all satellite-detected BrO “hotspots” are actually lower tropospheric halogen activation events. In-situ chemical ionization mass spectrometry (e.g. Liao et al., 2011; Pratt et al., 2013; Liao et al., 2014) and long path differential optical absorption spectroscopy (LP-DOAS) (e.g. Tuckermann et al., 1997; Pöhler et al., 2010) fail to capture the vertical extent of halogen activation, except in the case of limited aircraft-based campaigns (e.g. Neuman et al., 2010; Liao et al., 2012), and thus can not address questions about the total amount of halogen activation taking place at a given time. However, the Tackett et al. (2007) work implied that much of the halogen chemistry is occurring in the lowest ~ 200 m of the boundary layer.

Multiple axis differential optical absorption spectroscopy (MAX-DOAS) has the ability to retrieve vertical profiles of BrO in the lowest few kilometers, and thus can examine the variability of the vertical distribution of BrO over time (Frieß et al., 2011). The present work builds on the method of Frieß et al. (2011) by considering the BrO averaging kernels, which provide information on the sensitivity of these BrO measurements (Payne et al., 2009), to identify what observations are independent of the a priori assumed profile of BrO and creating a consistent timeseries of these data over a field campaign. Through this analysis, we identify two relevant properties of the BrO vertical profile, the partial vertical column density (VCD) of BrO in the lowest 200 m (termed VCD_{200m}) and the lower-tropospheric partial VCD (termed LT-VCD). The present work explores the dependence of these BrO profile properties on environmental factors to investigate activation of BrO and its propagation outside of the near surface layer over time. This present work focuses on measurements occurring near Barrow, Alaska, during the Bromine, Ozone, and Mercury Experiment (BROMEX) campaign (Nghiem et al., 2013) from 6 March to 15 May 2012. The primary MAX-DOAS

observations were made from the roof of the Barrow Arctic Research Center (BARC) building at 71.325° N, 156.668° W, which is about 6 km northeast of the city of Barrow, Alaska, [with a viewing azimuth of 27 degrees east of true north.](#)

2 Methods

2.1 MAX-DOAS measurements

Multiple-Axis Differential Optical Absorption Spectroscopy (MAX-DOAS) probes vertical distributions of trace gases above a measurement site through a combination of [spectroscopic](#) measurements of scattered sunlight and modeling of vertical profiles consistent with those observations (Hönninger et al., 2004). The instrument measures spectra of scattered sunlight in a region where the molecule of interest absorbs as a function of elevation angle of a telescope receiving the light. Measurements at all elevation angles contain absorption features due to stratospheric and higher tropospheric gases, and because most sunlight is scattered in the lower atmosphere, these stratospheric absorption features are common to observations at all elevation angles. Measurements at low elevation angles contain enhanced absorption for gases present near the ground, due to the tangent geometry of the light's final path to enter the telescope at a low elevation. Therefore, analysis of the relative absorption spectrum comparing light at low elevation angles to high elevation angles provides high sensitivity to near-ground absorbers with greatly reduced sensitivity to stratospheric and upper tropospheric gases.

The instrument used in this study is similar to the one described in Carlson et al. (2010) with a few improvements. In this study, we measured scattered sunlight using a QE-65000 (Ocean Optics) spectrometer with spectral range from 309–397 nm and optical resolution of 0.39 nm full width at half maximum. This new spectrometer is improved by using a thermoelectrically cooled detector, stabilized at -15°C . The spectrometer optical bench is heated to 38°C , [with a standard deviation of 0.6 degrees over the full campaign](#), to improve optical alignment stability. Another improvement of the instrument is the use of a MEMS tiltmeter

(SignalQuest SQ-SI-360DA-3.3R-HMP-HP-IND-S) mounted on the moving telescope that directly measures the elevation angle of the observation. The scan pattern measures scattered sunlight at elevation angles of 90° (zenith), 20° , 10° , 5° , 2° , and 1° over a period of approximately 30 min.

We used QDOAS software (Fayt et al., 2011) to fit the relative absorption spectrum between near temporally coincident low elevation and zenith observations to a linear combination of possible absorbing spectra to quantify the differential slant column density (dSCD) of each absorbing gas at each elevation angle. We performed this analysis in the wavelength window between 346 and 364 nm. The absorber cross sections are detailed in Table 1 and are convoluted with an instrumental [transfer function](#) measured from the 334 nm line of a low pressure mercury lamp. In addition to gaseous absorbers, we include a third-order polynomial to account for Rayleigh and Mie scattering by gases and particles in the atmosphere, and a spectral offset to account for stray light within the spectrometer. The mean residual root mean square (RMS) of our dSCD retrieval was 3.9×10^{-4} . Data collected during low sight conditions (solar zenith angle $> 85^\circ$), $\text{RMS} > 10^{-3}$, or when frost is detected on the instrument's optical window are discarded. The dSCD fitting errors (1σ) over the campaign average 1.9×10^{13} molecules cm^{-2} for BrO and 5.1×10^{41} molecules² cm^{-5} for O₄. [The sensitivity of the RMS and dSCD errors to elevation angle was small \(\$< 15\%\$ \) and is documented in the supplemental material.](#)

2.2 Retrieval of vertical profiles

Retrieval of trace gas vertical profiles from dSCD data is a two-step procedure. First, we determine the aerosol particle extinction vertical profile from O₂ [collisional dimer \(O₄\)](#) dSCD measurements using an optimal estimation procedure detailed in Frieß et al. (2006) and briefly described here. The observed O₄ dSCD values are strongly dependent on atmospheric visibility and light scattering, which we are able to deduce because we know the vertical profile of O₄. Measured O₄ dSCDs are compared to values modeled using the SCIATRAN radiative transfer model (Rozanov et al., 2005), which depend on a variable aerosol particle extinction profile and static parameters such as the viewing geometry and

aerosol particle light scattering properties. ~~Because the measurement~~ Assumptions made about the aerosol optical properties are set to values typical for clean ice crystals, following the procedures detailed in Frieß et al. (2011). Because the measured O_4 data alone do not provide enough information to retrieve the profile, we used an assumed a priori profile ~~is required~~ to further constrain the solution, as described by Rodgers (2000). We used a variable a priori profile that peaks at the surface and exponentially decays with altitude. Initially, the profile peaks at the surface with an aerosol particle extinction value of 0.05 km^{-1} and exponentially decays with a scale height of 1 km. The initial a priori covariance matrix is constructed with the diagonal elements being 3 times the a priori extinction and the off-diagonal elements being set to 0. The a priori covariance matrix is changed with every iteration (Frieß et al., 2006). In following iterations, the a priori is set to the retrieved profile and smoothed using a boxcar average with a width of 300 m (Frieß et al., 2006). The final output of this first step is a vertical profile of aerosol particle extinction.

The procedure to retrieve the BrO profile from BrO dSCD measurements is described in detail in Frieß et al. (2011). Briefly, we used the above-retrieved aerosol particle extinction profiles as input to a Monte Carlo radiative transfer model (McArtim, Deutschmann et al., 2011) that simulates BrO dSCDs as a function of a variable BrO vertical concentration profile. The vertical profile of BrO is varied to give best fit to the BrO dSCD observations, again by optimal estimation. In the case of BrO, the a priori profile peaks at the surface with a value of 10 pmol mol^{-1} and exponentially decays with a scale height of 400 m. The result of the second step is the average BrO mixing ratio every 100 m from the ground to an altitude of two kilometers. An example of the retrieved profile is shown in green in Fig. 1. Note that while our general retrieval uses a 400 m scale height for the a priori profile of BrO, Fig. 1 also includes the effect of modifying the a priori profile to have a different (1000 m) scale height (dashed blue line), as described below.

2.3 Information content of the profile

The retrieved BrO profiles contain average mixing ratios in twenty 100 m thick layers from the surface to 2 km; however, they are based on only five low-elevation spectral measure-

ments of BrO dSCD. Therefore, it is clear that our observations contain less information about the true vertical profile than is represented in Fig. 1. The optimal estimation method used the assumed a priori information to constrain the fit in the absence of further information, but the actual vertical profile of BrO is not known. In fact, the results of this study indicate that both the BrO abundance and vertical profile shape vary over time. Therefore, the full profile, as retrieved by optimal estimation, lends itself to overinterpretation of the observations and we seek to find a method to determine the actual information content, as well as reduce the number of derived properties to **more accurately** reflect the true observations more accurately.

As described in Rodgers (2000), the retrieved profile contains true profile information as well as a bias toward the assumed a priori profile. The extent to which the retrieved profile depends on the dSCD measurement data is determined by examining the averaging kernel matrix. An example of the BrO averaging kernels for a MAX-DOAS retrieval is given in the left panel of Fig. 2. If the value of the diagonal element of the averaging kernel at some altitude were unity (1), it would indicate that all of the information content at that layer is constrained by observational data and none of the information at that altitude comes from the a priori assumption. Non-zero off-diagonal elements indicate that the retrieved parameter in that layer is not independently resolved and is influenced by results in other layers. There are two peaks in the averaging kernels, one at the surface and one aloft at an altitude of about 300 m. We can understand the sharp peak at the surface easily because MAX-DOAS spectroscopy always has highest sensitivity and greatest vertical resolution in the layer in which the observer resides. In this study, that is the lowest portion of the boundary layer when the measured photons traverse a path tangent to the ground prior to being detected. The broader peak aloft, centered at about 300 m, in this example, comes from the observations at higher elevation angles, which view through those aloft layers, but do not provide enough information to independently resolve mixing ratios in 100 m thick layers at higher altitudes. The trace (sum of diagonal elements) of the averaging kernel matrix gives the degrees of freedom (DOF), which represents the total number of independent pieces of information contained in the retrieval. For BrO retrieval using this technique and our instru-

mentation, the distribution of DOF is well fit by a Gaussian function, with a mean of 2.0 DOF and $\sigma = 0.27$. Our retrievals also exhibit a distinct lack of sensitivity to changes in individual 100 m layers at altitudes over 1000 m. The DOF for this example is 1.99, implying our retrieved profile contains two independent pieces of information, rather than the 20 we retrieved.

To illustrate the influence of our a priori assumptions, Fig. 1 also shows a retrieved profile with a different assumed BrO scale height, 1000 m instead of the normal 400 m assumption. The influence of a priori selection in the retrieved BrO mixing ratio in the lowest 200 m is minimal, showing that our instrument is most independent of a priori assumptions about the BrO profile near the surface. However, aloft the effects of a priori selection are clearly visible. What appeared to be a relatively sharp peak at ≈ 650 m when the 400 m a priori was assumed becomes much broader with the 1000 m assumed scale height. Note that both optimally estimated results fit the observational data with similar figure of merit (χ^2), so the difference in profile is not due to poor fitting in one case or the other, but instead a consequence of the a priori influencing the resultant BrO profile.

2.4 Reduction of the full profile

A method for mapping the BrO profile retrieved on a fine grid to a course grid, such that the DOF are represented as physical quantities without the influence of a priori information is outlined in von Clarmann and Grabowski (2007). They suggest moving to a variable coarse altitude grid where one would select grid points such that each grid point would represent one DOF. The lowest layer's upper boundary would be determined by summing the diagonal elements of the BrO averaging kernel matrix until the sum reached one. This process would be repeated to obtain additional layer boundary altitudes. However, this approach is not practical for long-term time series analysis because the vertical resolution would vary over time, making comparisons difficult. As a compromise, we calculated coarse grid points by examining the ensemble of profile retrievals over this campaign and splitting them into two layers by determining the average altitudes such that each layer contains one degree of freedom. This method led us to represent one degree of freedom as the abundance of

BrO from surface through 200 m, and another as the abundance of BrO from 200 m to 2.0 km. These two layers differ in thickness due to the enhanced vertical resolution at the surface and decreased vertical resolution aloft, so we choose to represent the abundance in each layer as a partial vertical column density (VCD) within each layer. The vertical column density is also useful because satellite total column retrievals of BrO use the same unit of abundance. Thus, our two quantities ($VCD_{200\text{m}}$ and VCD_{Aloft}) represent a surface layer VCD and a lofted layer VCD respectively.

Figure 1 shows the partial VCDs in each layer derived from the grid coarsening procedure, for an example retrieval. While the profiles look fairly different, particularly aloft, the partial VCDs in each of the layers are only around ten percent different from each other as an effect of the assumed a priori profile. This example shows how the grid coarsening procedure gives results that are less dependent on the unknown but assumed BrO profile.

Payne et al. (2009) describe how to calculate ~~the averaging kernel for the general averaging kernels for a~~ coarsened grid, ~~and an~~ which we applied to our BrO retrievals. An example of the coarse grid BrO averaging kernels is shown in Fig. 2. The DOF has been reduced, meaning we have lost some information in the transfer to a coarse grid, however, both parameters have averaging kernels that peak within the desired layer and at a value close to unity, implying most of the information comes from the observations. Payne et al. (2009) suggested a cutoff of 0.7 for the diagonal element of the averaging kernel within a layer as sufficiently close to unity to consider the observations as derived from the data and independent of the a priori assumption. We chose to adopt the same cutoff of 0.7 degrees of freedom in the present work.

The right panel of Fig. 3 shows the dependence of the aloft information content on the aerosol optical depth. As Fig. 3 shows, our ability to retrieve information beyond the near surface layer is heavily dependent on the aerosol optical depth, while our ability to retrieve information near the surface is less influenced by aerosol particles. In addition to the degrees of freedom cutoff, over the course of the campaign we also observed limited times when the retrieved aerosol optical depth was large, in excess of 2, which indicates that the visibility is insufficient to obtain an accurate profile of aerosol particle extinction or BrO. Dur-

ing these periods, we do not consider the VCD_{Aloft} due to insufficient degrees of freedom, and we also disregard the $VCD_{200\text{m}}$. This approach is consistent with methods used in comparison of near-surface MAX-DOAS and LP-DOAS BrO measurements by Frieß et al. (2011).

5 When both quantities have averaging kernels peaking ~~about~~ at 0.7 or higher, we refer to the sum as the lower tropospheric vertical column density (LT-VCD). It is important to note that this quantity does not represent a new degree of freedom, as it is derived from and not independent of the other two measurements. To evaluate the vertical distribution of BrO, we examine the ratio of the $VCD_{200\text{m}}$ /LT-VCD as well as the total amount of observed
10 activation in the lower tropospheric (LT-VCD) and near surface amounts ($VCD_{200\text{m}}$). A time series of these three quantities, along with the aerosol optical depth over a portion of the campaign is presented in Fig. 4. The rest of the timeseries can be found in the supplemental material. This timeseries will be discussed below, but here we note that the fraction of BrO in the lower layer varies between a few percent and up to $\approx 80\%$. The a priori profile, exponentially decaying with a scale height of 400 m, would have a constant fraction of BrO
15 in the lowest 200 m, approximately 34 %. It is clear that the data show substantially more vertical profile variability than the assumed profile. Therefore, we use the grid-coarsened data to represent the information content from our MAX-DOAS observations over this long time period.

20 An additional advantage of the coarsened grid is that the resulting quantities are less sensitive to errors in forward model parameters. As an example, the aerosol particle extinction profile required for the BrO retrieval is also an optimally estimated quantity, and not the true profile. This will introduce errors in the BrO retrieval. We estimated the errors in BrO retrieval due to uncertainties in the aerosol particle extinction profile by examining the sensitivity of the BrO retrieval to perturbations in the aerosol particle extinction profile. To do so, we retrieved BrO profiles from the same BrO dSCD data over an ensemble of varying aerosol particle extinction profiles observed during this study, and examined the resulting variability in the quantities further discussed in this manuscript. We found that the LT-VCD was not heavily influenced by changes in the aerosol profile, with an estimated error

of 4.6% (1 Sigma), which is lower than error introduced by uncertainties in the BrO dSCD measurements. The $VCD_{200m}/LT - VCD$ ratios retrieved have an estimated error of 4.9% (1 Sigma). Thus, it is reasonable to conclude that the vertical structure of halogen events retrieved using MAX-DOAS at Barrow are not substantially influenced by errors in aerosol retrieval.

2.5 Other field sites

Figure 5 shows locations for various measurements used in this study. While this paper focuses on MAX-DOAS measurements from the BARC building, Sect. 3.3 makes use of data from multiple field sites to evaluate the effectiveness of our near-surface BrO retrieval. We deployed a second MAX-DOAS instrument, IL1, at 71.355° N, 155.668° W, which is on landfast sea ice east of the BARC building with a viewing azimuth of 2 degrees east of true north. This instrument is the same as the instrument on the BARC building, with the exception of the spectrometer, which is an Avantes (AvaSpec-ULS2048x64-USB2) with spectral range from 291–457 nm and optical resolution of 0.37 nm full width at half maximum. This spectrometer is housed in a highly insulated enclosure that is stabilized at 10 °C using air cooling. We analysed MAX-DOAS data from IL1 using the techniques previously described. For IL1, the mean RMS of our dSCD retrieval is 5.2×10^{-4} . IL1 dSCD fitting errors (1σ) over the campaign average 9.7×10^{12} molecules cm^{-2} for BrO and 1.7×10^{42} molecules² cm^{-5} for O₄.

Additional surface BrO measurements were conducted near Barrow, AK from 12–28 March 2012 at a measurement site about 5 km inland (71.275° N, 156.641° W), shown in Fig. 5, using a chemical ionization mass spectrometer (CIMS), described by Liao et al. (2011). Using hydrated $I^-(I \cdot (H_2O)_n)^-$ as the reagent ion, BrO was measured at mass 222 ($I^{79}\text{BrO}^-$) and 224 ($I^{81}\text{BrO}^-$). Background measurements were performed every 15 min by passing the air flow through a glass wool scrubber. Br₂ calibrations were performed every two hours by adding Br₂, from a permeation source, in 21 mL min^{-1} N₂ to the air flow. A relative sensitivity of BrO (mass 224) relative to Br₂ (mass 287) of 0.47 was utilized for

BrO calibration (Liao et al., 2011). The presence of BrO was confirmed by the ratio of mass 222/mass 224 (background-subtracted raw signals), calculated to be 1.01 ($R^2 = 0.94$).

For a measurement cycle of 10.6 s, mass 224 ($^{81}\text{BrO}^-$) was monitored for 0.5 s, giving a 5 % duty cycle. The 3σ limit of detection for BrO, using mass 224, was calculated to be 1.6 pmol mol $^{-1}$, on average for a 2.8 s integration period (corresponding to 1 min of CIMS measurements). Since the variance in the background is likely due to counting statistics (Liao et al., 2011), the limit of detection for 30 min averaging is estimated at 0.3 pmol mol $^{-1}$. The uncertainty in the reported BrO concentrations was calculated to be 30% + 0.3 pmol mol $^{-1}$. Additional sampling details are provided in the Supplementary Information.

To examine relationships between BrO and ozone, as well as local meteorology, we used ozone data and meteorological data from the National Oceanic and Atmospheric Administration (NOAA) Earth Systems Research Laboratory/Global Monitoring Division (ESRL/GMD). These data included near surface ozone mixing ratios, temperature, wind speed, wind direction, pressure, as well as twice daily meteorological balloon sounding data from the Barrow Airport (PABR), which was used to calculate the temperature gradient (dT/dz) near the surface. These soundings take place twice daily, at 00:00 UTC, which is in the daylight hours, 15:00 AKST, at Barrow, and 12:00 UTC, which is at night and not used in this study.

3 Results

3.1 Relationship between visibility and retrieval information content

The ability of MAX-DOAS to observe BrO beyond the near surface layer is heavily influenced by the optical properties of the atmosphere (e.g. visibility) at the time of the measurement. The methods outlined above allow us to identify times when MAX-DOAS measurements are sensitive to BrO beyond the near surface layer and restrict our further analysis of the vertical distribution of BrO to these periods. Figure 3 details the relationship between

the aerosol optical depth and the information content of the measurement. As the aerosol optical depth increases, the ability to observe the full LT-VCD sharply decreases. As seen in Fig. 3, we can retrieve the full LT-VCD 50 % of the time. We excluded periods where we are unable to fully observe the LT-VCD from further analysis of the vertical distribution of BrO.

3.2 Influence of ozone

Ambient ozone levels influence the partitioning of reactive halogen species between atomic (e.g. Br atoms) and oxide (e.g. BrO) forms. MAX-DOAS measurements ~~observe~~ retrieve only BrO and thus only constrain one component of BrO_x (BrO + Br). Therefore, it is important to consider effects of gas-phase partitioning of BrO_x on subsequent conclusions about halogen activation. ~~To examine this influence, we examined ozone data and meteorological data from Barrow, provided by the National Oceanic and Atmospheric Administration (NOAA) Earth Systems Research Laboratory/Global Monitoring Division (ESRL/GMD).~~ Under ordinary ozone conditions (ozone mixing ratios of 30–40 nmol mol⁻¹), BrO will make up the majority of BrO_x; however, as ozone levels approach zero (a common occurrence during the ozone depletion event season), our BrO-only measurements could be insufficient to observe reactive halogens, as shown in Helmig et al. (2012). We term this effect “ozone titration” and seek to avoid interpretation of BrO data below some threshold where the effect dominates. The threshold depends on the photolysis rate of BrO, which varies depending on cloud cover and solar zenith angle, among other factors. For the purposes of this study, we used an ozone threshold of < 1 nmol mol⁻¹ to identify potentially titrated air masses to exclude from further analysis (Simpson et al., 2007a). Figure 4 shows times when ozone is below 1 nmol mol⁻¹ as shaded in grey. Note that, for the most part, BrO LT-VCD and VCD_{200m} are small during ozone titration, as would be expected, and also observed by Neuman et al. (2010).

3.3 Performance of surface BrO retrieval

To evaluate the effectiveness of the BrO retrieval near the surface, we used in situ BrO measurements made using chemical ionization mass spectrometry (CIMS) to evaluate our retrieval in the lowest 100 m. While the mixing ratio in the lowest 100 m is not one of the grid coarsened quantities, because MAX-DOAS is most sensitive near the surface, the near surface mixing ratio has similar information content to the VCD_{200m} while minimizing the effects of vertical averaging on comparison with in situ measurements. Figure 6, shows a timeseries of the average BrO mixing ratio retrieved in the lowest 100 m by MAX-DOAS (Red) and in situ CIMS measurements taken 1 m above the snow pack (Green). The error associated with 100 m mixing ratios retrieved using MAX-DOAS varies depending on the state of the atmosphere at the time of the measurement. The error associated with each retrieval is determined by examining the sensitivity of the retrieval to dSCD errors associated with the measurement data (Rodgers, 2000). Average errors (2σ) were $4.2 \text{ pmol mol}^{-1}$ for our MAX-DOAS measurements. Uncertainties are estimated at $30\% + 0.3 \text{ pmol mol}^{-1}$ for CIMS measurements. Because the CIMS instrument was also used to conduct snow chamber experiments during BROMEX, and MAX-DOAS observations are daytime only, there are some gaps in the timeseries shown in Fig. 6.

Because CIMS measures in one discrete location just above the snowpack, while MAX-DOAS measurements are spatially averaged, both horizontally over 10–20 km and vertically over approximately 100 m, it is expected that large changes in the environment in the view direction of the MAX-DOAS will cause differences between the CIMS and MAX-DOAS observations. We also expect that ~~given the snowpack~~ because the snowpack is a source of Br_2 (Pratt et al., 2013), there may be a significant near-surface BrO gradient. Figure 6 shows a time series of near surface BrO measurements from the CIMS, as well as MAX-DOAS measurements at the BARC building. Since the BARC data originate at $\sim 4 \text{ m}$, and average over the lowest 100 m, we might expect ~~these MAX-DOAS~~ data to be lower than the CIMS, which measures closer to the snowpack. Figure 6 shows agreement for the majority of concurrent observations, excluding the period shaded in gray, during which we

observed substantial gradients in the near surface amounts of BrO at IL1 (blue line) and BARC (red line), which could explain discrepancies between the MAX-DOAS measurements at the BARC building and the CIMS measurements. [Figure 5 shows the MAX-DOAS instrument on the BARC building views across a large lead that is not sampled by the IL1 view direction, which could potentially explain a local gradient in BrO.](#) Figure 7 shows the overall correlation between MAX-DOAS measurements at the BARC building and the CIMS, each averaged to hourly bins. Points occurring during the gray period marked on Fig. 6 are shown in red open circles. Outside times of disagreement between the two MAX-DOAS instruments, shown in gray on Fig. 6, the correlation observed between the DOAS data and CIMS data is $R = 0.70$, which is similar to correlation of MAX-DOAS and long path DOAS measurements observed by Frieß et al. (2011). The CIMS and LP-DOAS were previously shown to agree well, particularly during times of moderate wind speeds ($3\text{--}8\text{ m s}^{-1}$) and low NO ($< 100\text{ pmol mol}^{-1}$) (Liao et al., 2011).

3.4 Relationship between amount observed and vertical distribution of BrO

Figure 4 shows the timeseries of the $\text{VCD}_{200\text{m}}$ and LT-VCD. LT-VCD values over the course of this study ranged from ~~0~~-zero to 8×10^{13} molecules cm^{-2} with an average of 1.46×10^{13} molecules cm^{-2} and the top quartile being above 2.0×10^{13} molecules cm^{-2} , which we will later consider to be “highly activated” events. LT-VCD retrieval errors had a mean of 3.9×10^{12} molecules cm^{-2} over the course of the campaign. Figure 8 shows the percentage of the LT-VCD present in the lowest 200 m ranges from shallow layer events observed primarily below 200 m to distributed column events that are also observed at higher altitudes. The third panel of Fig. 4 shows a timeseries of this ratio. Surface layer percentages over this campaign ranged between ~~0~~-near zero and 80 %, with the highest LT-VCD observed during distributed column events with ~~lowest-200~~ $\text{VCD}_{200\text{m}}/\text{LT} - \text{VCD}$ percentages of around 10 %. As the coloration of Fig. 8 indicates, high near surface mixing ratios do not always imply high LT-VCD. In most cases, high LT-VCDs are associated with distributed column events.

3.5 Dependence on local meteorology

To examine atmospheric stability, we ~~obtained used~~ meteorological balloon sounding data ~~from the Barrow Airport (PABR)~~ to calculate the temperature gradient (dT/dz) near the surface. We calculated the slope of a linear fit of the first three data points of the sounding. Typically, the first three sounding points corresponded to measurements between the surface and, which typically corresponds to an altitude range from the surface to 200 m altitude. Soundings take place twice daily, at 00:00, which is in the daylight hours, 15 AKST, at Barrow, and 12:00 above ground level. Because MAX-DOAS data are daylight only, to compare our ~~half-hourly~~ BrO measurements with the sounding data, we used daily averages of the fraction of near-surface BrO to LT-VCD from each day and examined the relationship between daily averaged ratios and the corresponding temperature gradients obtained from the local daytime sounding. Figure 9 shows the relationship between these two quantities. This box and whisker plot is generated by splitting daily observations into three bins of about 20 days each. The median is given by the red lines and shows the general trend that more stable atmospheres with inverted temperature structures (right bin) have more BrO present in the surface layer, while unstable atmospheres (left bin) tend to have BrO more distributed throughout the lower troposphere. ~~The short diurnal time scales of~~ Given that the temperature gradient ~~do not allow the use of~~ likely varies at a higher rate than captured by daily sounding data ~~to determine the functional relationship between the temperature gradient and where an event would fall on the spectrum of,~~ there is likely to be a smoothing effect that worsens the relationship between BrO vertical ~~distributions~~ distribution and local stability. However, a clear relationship is still observed in Fig. 9.

The left panel of Fig. 10 illustrates the relationship between surface temperature and the amount of BrO in the near surface layer. On average, there is a higher fraction of BrO in the near surface layer when temperatures are below -25°C , with more distributed column BrO events being observed aloft at higher temperatures. Figure 10 (right panel) shows that activation events in excess of 2×10^{13} molecules cm^{-2} occur at various temperatures.

Additionally, we examine the response of both the total activation as measured by the LT-VCD and the vertical distribution of BrO to **changes in** wind speed. Figure 11 (left panel) shows LT-VCD values in excess of 2×10^{13} molecules cm^{-2} at various wind speeds and, as shown by the red line, there is no obvious relationship between the LT-VCD and wind speed. The observed lack of dependence of the LT-VCD on wind speed and temperature is consistent with the observations of Halfacre et al. (2014). However, the vertical distribution of BrO is influenced by windspeed. The right panel of Fig. 11 shows the majority of shallow layer events occur during times when wind speeds are between $3\text{--}6 \text{ m s}^{-1}$. Additionally, events at wind speeds in excess of 8 m s^{-1} tend to be more distributed throughout the column.

4 Discussion

4.1 Role of atmospheric stability

The third panel of Fig. 4 shows the vertical structure of BrO was highly variable over the course of this study. Events range from shallow layer events where most of the observed BrO is found in the lowest 200 m to distributed column events with BrO present throughout the lower troposphere. Figure 8 shows the highest observed LT-VCDs were observed during distributed column events while shallow layer events, despite their enhanced near surface mixing ratios, did not result in large amounts of total activation, as measured by the LT-VCD. This **finding** points out the difficulty in comparing satellite BrO column retrievals with surface observations (e.g. Sihler et al., 2012). Figure 9 shows the vertical distribution of BrO is clearly influenced by the observed atmospheric stability. During times of inversion, bromine activation events tend toward the shallow layer end of the spectrum. When the atmosphere is less stable, events tend to be distributed throughout the column. Given that this study only uses daily sounding data, and knowing that convective mixing has a strong diurnal variability, it is likely this study represents a lower bound on the influence of atmospheric stability.

Ozone depletion events have been shown to be highly variable in vertical extent (e.g. Bottenheim et al., 2002b; Tarasick and Bottenheim, 2002; Jones et al., 2010; Oltmans et al., 2012; Helmig et al., 2012). More recently, Moore et al. (2014) observed that opening of leads enhanced vertical mixing leading to a recovery of ozone and gaseous elemental mercury in the near surface layer. This mixing potentially impacts the vertical distribution of halogens as well. McElroy et al. (1999) observed high total tropospheric BrO events and interpreted them as arising from convective vertical mixing associated with open leads that brought near-surface BrO to the free troposphere. Therefore, it is reasonable that vertical mixing or hindered mixing due to atmospheric stability affects the vertical structure of BrO.

Seasonal and temperature trends are consistent with atmospheric stability's influence on the BrO vertical structure. Figure 10 shows that at lower temperatures, which are more prevalent early in the season, events tend to be observed in shallow layers and transition to more vertically distributed as the surface temperature increases. These observations are consistent with the idea that the distribution of BrO is primarily influenced by atmospheric stability.

The right panel of Fig. 10 indicates that significant activation events happen at a variety of temperatures. Pöhler et al. (2010) observed there was a linear trend of decreasing near surface maximum BrO, observed with LP-DOAS, as temperature increased up to -15°C . When examining the whole LT-VCD, rather than a near surface concentration, this trend does not appear, however, Fig. 10 (left panel) shows a distinct preference toward near surface distributions of BrO at lower temperatures, which as Fig. 8 shows, often contain higher near surface amounts of BrO, but have a lower overall LT-VCD. The observation of Pöhler et al. (2010) of decreasing surface BrO mixing ratio at higher temperatures could therefore reflect increased vertical mixing of surface-sourced BrO that dilutes the surface concentration upon warming rather than being indicative of decreased halogen activation chemistry at higher temperatures. Figure 12 illustrates the diurnal behavior of both the LT-VCD, shown in blue, and the $\text{VCD}_{200\text{m}}$ shown in red. Boylan et al. (2014) observed diurnal boundary layer growth at Barrow in 2009, although this was less pronounced during times of strong inversion. The $\text{VCD}_{200\text{m}}$ observed on in

Fig. 12 is similar to surface concentration data observed by Pöhler et al. (2010) as well as Stutz et al. (2011). Stutz et al. (2011) suggest this pattern is indicative of snow-sourced reactive bromine diluting through a growing boundary layer. The link between atmospheric stability and the vertical distribution of BrO demonstrated in this work supports the idea that the diurnal cycling observed is due to dilution of snow-sourced reactive bromine. The MAX-DOAS observations of the present study also allow observation of the BrO LT-VCD, which Fig. 12 shows increases to a peak in the late afternoon, ~~mirroring typical diurnal boundary layer growth. Therefore, the diurnal pattern of the vertical profile of appears to reflect boundary layer dynamics. The observation of of decreasing surface mixing ratio at higher temperatures could therefore reflect increased vertical mixing of surface-sourced~~ which is not fully explained by dilution of a surface source because dilution would leave the LT-VCD unchanged. This growth in LT-VCD with increased mixing was also observed in the modeling work of Toyota et al. (2014). Potential explanations for this observed growth in the LT-VCD include an enhancement of reactive bromine production in the snowpack due to increased sunlight, enhanced activation of bromine occurring aloft, potentially due to heterogeneous recycling on aerosol particles, or an increased ~~BrO that dilutes the surface concentration upon warming rather than being indicative of decreased halogen activation chemistry at higher temperatures~~ lifetime aloft.

4.2 Role of wind speed

Figure 11 (left panel) shows that activation events with BrO LT-VCDs in the top quartile occur across a spectrum of wind speeds, rather than at just the low surface wind speeds associated with stable boundary layers, or high wind speeds associated with blowing snow events. The right panel of Fig. 11 shows a peak in shallow layer events between 3–6 m s⁻¹ suggesting that some ventilation of the snowpack, which has been shown to be an effective source of Br₂ (Pratt et al., 2013), is required for the release of BrO during shallow layer events. For the most part, observed wind speeds exceeding 8 m s⁻¹, led to vertically distributed events, but beyond that there is little evidence to support the need for high winds or blowing snow to sustain halogen activation aloft, consistent with the conclusions of Halfacre

et al. (2014). This [finding](#) suggests that, during the course of this study, high wind events and blowing snow were not required to observe significant halogen activation. Activation events in the top quartile were observed across a range of wind speeds, particularly at more moderate wind speeds, with 66 % of highly activated events occurring at wind speeds between 3 and 8 m s⁻¹. This distribution suggests that enhanced ventilation of the snowpack, and subsequent vertical mixing of snowpack-influenced airmasses, is likely responsible for the majority of elevated LT-VCDs observed over the course of this study.

Jones et al. (2009) and Yang et al. (2010) rely on satellite observations of BrO rather than ground-based measurements to draw conclusions about the role of wind in halogen activation events. The differing viewing geometry ~~potentially becomes an issue~~ [could potentially affect the interpretation of the data](#) when clouds are present, as shallow layer events occurring below clouds would potentially be masked from the satellite view, but observable with ground-based MAX-DOAS. In contrast, BrO above a cloud that would be potentially [seen-observed](#) by a satellite would not be detected by ground-based MAX-DOAS, ~~although the profile reduction procedure should minimize these issues~~. Sihler et al. (2012) observed that satellite measurements could underestimate the amount of BrO during shallow layer events, implying events with distributed column vertical structure are more likely to be satellite detectable. This idea that shallow layer events may not be satellite detectable is also supported by the modeling work of Toyota et al. (2014). Enhanced visibility of the larger in magnitude and more vertically distributed BrO events could potentially explain why satellite remote sensing of BrO may show ~~an apparent a~~ [a](#) relationship to wind speed. These differences should be considered when trying to resolve differences between ground-based and satellite-based measurements.

4.3 Relationship between activation and aerosol particles

The near-surface aerosol particle extinction retrieved from our MAX-DOAS measurements is a proxy for suspended particulate surface area that enhances recycling of halogens, allowing us to examine the relationship between BrO and aerosol particles. The left panel of Fig. 13 shows an increase in the VCD_{200m} with increased aerosol particle extinction,

while the right panel shows that the relationship between aerosol particles and the LT-VCD is less clear. Laboratory studies (e.g. Huff and Abbatt, 2000; Wren et al., 2013) and field studies (e.g. Pratt et al., 2013) indicate that pH is an important control on heterogeneous recycling of halogens. Although we are unable to determine the pH of these particles by MAX-DOAS, we simply point out that, not only is the presence of suspended surface area important, but also that the chemical composition of that surface is likely a controlling factor.

Prior to using these data to consider the role of blowing snow in observed halogen activation during this study, it is important to point out that the lack of LT-VCD observations at high aerosol optical depth, shown in Fig. 3, could potentially lead to preferential exclusion of blowing snow events from further analysis of the total amount of activation as measured by the LT-VCD. To examine the potential impacts of data exclusions, we examined the amount of data at high wind speeds discarded by the application of methods described in Sect. 2.4. Of the 147 measurements occurring when wind speeds exceeded 8 m s^{-1} threshold used for blowing snow in Jones et al. (2009), 86 of those were rejected due to insufficient information content. If one were to presume these were all blowing snow events and belonged in the top quartile of observed activation events, they would represent 9.6 % of LT-VCD observations and 29 % of events where the LT-VCD exceeded $2 \times 10^{13} \text{ molecules cm}^{-2}$. Therefore, we find that the exclusion of low visibility data at high wind speed could only explain a small fraction of halogen activation events. While we end up discarding a significant amount of data, these filtered data still provide a fair idea of the role of high wind events, blowing snow or otherwise, in halogen activation.

While the increase in $\text{VCD}_{200\text{m}}$ during times of high aerosol particle extinction supports blowing snow as one source of halogens, ~~it is interesting to note that LT-VCD above 2×10^{13} often occur at wind speeds well below typical thresholds for blowing snow (8,), as shown in the left panel of Fig. 11. Additionally,~~ examining the dependence of the aerosol particle extinction on wind speed, shown by the coloration in the left panel of Fig. 13, shows there is no apparent increase in extinction at high wind speeds, which we would expect if blowing snow was the only source of particulate surface area for halogen recycling. The observation of aerosol particle extinction values in excess of 10^{-1} km^{-1} across a variety

of wind speeds suggests that blowing snow is not the only source of the aerosol particles needed to sustain halogen activation aloft.

Additionally, it is interesting to note that LT-VCD above 2×10^{13} molecules cm^{-2} often occur at wind speeds well below typical thresholds for blowing snow (8 m s^{-1} , Jones et al., 2009), as shown in the left panel of Fig. 11. While blowing snow is not simply a univariate function of wind speed (Sturm and Stuefer, 2013), given 9% of observations occurred when wind speeds exceeded 8 m s^{-1} and halogen activation events in excess of 2×10^{13} molecules cm^{-2} occurred 25% of the time, immediate activation during blowing snow events is not the sole driver of halogen activation over the course of this study, and likely some other aerosol particle source is required. Frieß et al. (2011) postulated that aerosol particles produced by sublimation of blowing snow could transport and increase observed aerosol particle extinction while also providing a suspended surface for the recycling of halogens aloft. Further, in the Arctic springtime, Hara et al. (2002) observed bromide loss from coarse sea salt particles and addition to fine sulfate particles, supporting the suggestion of bromine recycling on aerosol particles.

5 Conclusions

The methods described in this paper outline the reduction of vertical profiles retrieved from MAX-DOAS observations using optimal estimation to produce two quantities, the lower tropospheric vertical column density (LT-VCD), and the near surface vertical column density in the lowest 200 m ($\text{VCD}_{200\text{m}}$), that appropriately reflect the information content of ground-based MAX-DOAS measurements for timeseries analysis. Consideration of BrO averaging kernels and degrees of freedom resulting from optimal estimation validates that these quantities are most appropriate to express the two degrees of freedom observed. This method allows for identification of time periods when MAX-DOAS measurements contain information about BrO beyond the near surface layer, and evaluate how the vertical structure of BrO responds to various environmental factors. Application of these methods shows retrieval of

LT-VCDs by ground-based MAX-DOAS is highly dependent on visibility. During this study, we retrieved the LT-VCD 50 % of the time.

The vertical structure of BrO is highly variable, with the fraction of lower-tropospheric BrO in the lowest 200 m varying from near zero to nearly 80 %. The vertical distribution of activation events is clearly influenced by the atmospheric stability. This influence also manifests itself when examining the influence of temperature and seasonality. Later in the season, higher temperatures, and likely enhanced vertical mixing, tend to result in more BrO aloft than early in the season, where activation takes place in shallower layers. LT-VCD values in excess of 2×10^{13} molecules cm^{-2} occur across a variety of temperatures and wind speeds, but they are typically associated with distributed column events, rather than shallow layer events. Events that have larger observed near surface mixing ratios are typically of the shallow layer variety and do not typically have large amounts of BrO spread through the lower troposphere, potentially implying less overall ozone depletion and deposition of mercury from these events. This implies that both surface and upper profile measurements are necessary to appropriately identify the impact of environmental variables on O_3 depletion and Hg oxidation rates and extent.

The observed BrO $\text{VCD}_{200\text{m}}$ showed diurnal cycling, suggesting a surface snow source of reactive bromine diluting through an expanded boundary layer, which reflects the link between atmospheric stability and the vertical distribution of BrO. The observed growth in the LT-VCD during the day indicates the production, or lifetime of reactive bromine is not static, but production increases throughout the day, or losses decrease. The BrO $\text{VCD}_{200\text{m}}$ also showed an increase during times of high aerosol particle extinction, however the lack of a clear relationship between aerosol particle extinction and wind speed implies that blowing snow is not the sole source of aerosol particles needed for heterogeneous recycling of bromine aloft.

High wind events were not common over the course of this study. While high winds did lead to some of the highest measured columns of BrO, given the low frequency of these events, high wind events, blowing snow or otherwise, are not the sole driver of halogen ac-

tivation over the course of this study, suggesting that mechanisms requiring only moderate wind speeds (e.g. wind pumping) are important for halogen activation in the Arctic.

**The Supplement related to this article is available online at
doi:10.5194/acpd-0-1-2014-supplement.**

5 *Acknowledgements.* The research at the University of Alaska was supported by the National Aero-
nautics and Space Administration (NASA) Cryospheric Sciences Program (CSP), and partial finan-
cial support for MAX-DOAS analysis methods was provided by the National Science Foundation un-
der grant ARC-1023118. The Purdue group recognizes NSF support through grant ARC-1107695.
10 K. A. Pratt was supported by a NSF Postdoctoral Fellowship in Polar Regions Research. The Pur-
due group acknowledges field assistance from Kyle Custard (Purdue Univ.), David Tanner (Georgia
Tech), and L. Gregory Huey (Georgia Tech). The research at the Jet Propulsion Laboratory, Califor-
nia Institute of Technology, was supported by the NASA CSP. The authors gratefully acknowledge
Chris Moore for helpful discussions, as well as Alexei Rozanov from IUP Bremen for providing the
15 SCIATRAN radiative transfer code. The authors also wish to thank UMIAQ for logistical support, and
Bristow Air for providing a helicopter for the deployment of IL1.

References

- Abbatt, J. P. D., Thomas, J. L., Abrahamsson, K., Boxe, C., Granfors, A., Jones, A. E., King, M. D.,
Saiz-Lopez, A., Shepson, P. B., Sodeau, J., Toohey, D. W., Toubin, C., von Glasow, R., Wren, S. N.,
20 and Yang, X.: Halogen activation via interactions with environmental ice and snow in the polar
lower troposphere and other regions, *Atmos. Chem. Phys.*, 12, 6237–6271, doi:10.5194/acp-12-
6237-2012, 2012.
- Barrie, L. A., Bottenheim, J. W., Schnell, R. C., Crutzen, P. J., and Rasmussen, R. A.: Ozone de-
struction and photochemical reactions at polar sunrise in the lower Arctic atmosphere, *Nature*,
334, 138–141, doi:10.1038/334138a0, 1988.
- 25 Bottenheim, J. W., Fuentes, J. D., Tarasick, D. W., and Anlauf, K. G.: Ozone in the Arctic lower
troposphere during winter and spring 2000 (ALERT2000), *Atmos. Environ.*, 36, 2535–2544,
doi:10.1016/S1352-2310(02)00121-8, 2002.

[Boylan, P., Helmig, D., Staebler, R., Turnipseed, A., Fairall, C., and Neff, W.: Boundary layer dynamics during the Ocean-Atmosphere-Sea-Ice-Snow \(OASIS\) 2009 experiment at Barrow, AK, *Journal of Geophysical Research: Atmospheres*, 119, 2261–2278, doi:10.1002/2013JD020299, 2014.](#)

- 5 Carlson, D., Donohoue, D., Platt, U., and Simpson, W. R.: A low power automated MAX-DOAS instrument for the Arctic and other remote unmanned locations, *Atmos. Meas. Tech.*, 3, 429–439, doi:10.5194/amt-3-429-2010, 2010.
- Chance, K.: Analysis of BrO measurements from the global ozone monitoring experiment, *Geophys. Res. Lett.*, 25, 3335–3338, 1998.
- 10 Chance, K. V. and Spurr, R. J.: Ring effect studies: Rayleigh scattering, including molecular parameters for rotational Raman scattering, and the Fraunhofer spectrum, *Appl. Optics*, 36, 5224–5230, 1997.
- Deutschmann, T., Beirle, S., Frieß, U., Grzegorski, M., Kern, C., Kritten, L., Platt, U., Prados-Román, C., Pukite, J., Wagner, T., Werner, B., and Pfeilsticker, K.: The Monte Carlo atmospheric radiative transfer model McArtim: Introduction and validation of Jacobians and 3D features, *J. Quant. Spectrosc. Ra.*, 112, 1119–1137, doi:10.1016/j.jqsrt.2010.12.009, 2011.
- 15 Fan, S.-M., and Jacob, D. J.: Surface ozone depletion in Arctic spring sustained by bromine reactions on aerosols, *Nature*, 359, 522–524, doi:10.1038/359522a0, 1992.
- Fayt, C., De Smedt, I., Letocart, V., Merlaud, A., Pinardi, G., Van Roozendael, M., and Roozendael, M. V. A. N.: QDOAS Software User Manual, available at: <http://uv-vis.aeronomie.be/software/QDOAS/index.php> (last access: 10 March 2014), 2011.
- 20 Fickert, S., Adams, J. W., and Crowley, J. N.: Activation of Br₂ and BrCl via uptake of HOBr onto aqueous salt solutions, *J. Geophys. Res.*, 104, 23719–23727, doi:10.1029/1999JD900359, 1999.
- Foster, K. L., Plastridge, R. A., Bottenheim, J. W., Shepson, P. B., Finlayson-Pitts, B. J., and Spicer, C. W.: The role of Br₂ and BrCl in surface ozone destruction at polar sunrise, *Science*, 291, 471–474, 2001.
- Frieß U., Monks, P. S., Remedios, J. J., Rozanov, A., Sinreich, R., Wagner, T., and Platt, U.: MAX-DOAS O₄ measurements: a new technique to derive information on atmospheric aerosols: 2. Modeling studies, *J. Geophys. Res.*, 111, D14203, doi:10.1029/2005JD006618, 2006.
- 30 Frieß U., Sihler, H., Sander, R., Pöhler, D., Yilmaz, S., and Platt, U.: The vertical distribution of BrO and aerosols in the Arctic: measurements by active and passive differential optical absorption spectroscopy, *J. Geophys. Res.*, 116, D00R04, doi:10.1029/2011JD015938, 2011.

- Halfacre, J. W., Knepp, T. N., Shepson, P. B., Thompson, C. R., Pratt, K. A., Li, B., Peterson, P. K., Walsh, S. J., Simpson, W. R., Matrai, P. A., Bottenheim, J. W., Natcheva, S., Perovich, D. K., and Richter, A.: Temporal and spatial characteristics of ozone depletion events from measurements in the Arctic, *Atmos. Chem. Phys.*, 14, 4875–4894, doi:10.5194/acp-14-4875-2014, 2014.
- 5 Hara, K., Osada, K., Matsunaga, K., Iwasaka, Y., Shibata, T., and Furuya, K.: Atmospheric inorganic chlorine and bromine species in Arctic boundary layer of the winter/spring, *J. Geophys. Res.*, 107, 4361, doi:10.1029/2001JD001008, 2002.
- Helmig, D., Boylan, P., Johnson, B., Oltmans, S., Fairall, C., Staebler, R., Weinheimer, A., Orlando, J., Knapp, D. J., Montzka, D. D., Flocke, F., Frieß, U., Sihler, H., and Shepson, P. B.: Ozone dynamics and snow-atmosphere exchanges during ozone depletion events at Barrow, Alaska, *J. Geophys. Res.-Atmos.*, 117, D20303, doi:10.1029/2012JD017531, 2012.
- 10 Hermans, C., Vandaele, A., Coquart, B., Jenouvrier, A., Merienne, M. F., Fally, S., Carleer, M., and Colin, R.: Absorption bands of O₂ and its collision-induced bands in the 30 000–7500 cm⁻¹ wavenumber region, in: *IRS 2000: Current Problems in Atmospheric Radiation*, edited by: Smith, W. L. and Timofeyev, Y. M., Hampton, VA, Deepak, 639–642, 2001.
- Hönninger, G., von Friedeburg, C., and Platt, U.: Multi axis differential optical absorption spectroscopy (MAX-DOAS), *Atmos. Chem. Phys.*, 4, 231–254, doi:10.5194/acp-4-231-2004, 2004.
- Huff, A. K. and Abbatt, J. P. D.: Gas-phase Br₂ production in heterogeneous reactions of Cl₂, HOCl, and BrCl with halide-ice surfaces, *J. Phys. Chem. A*, 104, 7284–7293, doi:10.1021/jp001155w, 2000.
- 20 Jones, A. E., Anderson, P. S., Begoin, M., Brough, N., Hutterli, M. A., Marshall, G. J., Richter, A., Roscoe, H. K., and Wolff, E. W.: BrO, blizzards, and drivers of polar tropospheric ozone depletion events, *Atmos. Chem. Phys.*, 9, 4639–4652, doi:10.5194/acp-9-4639-2009, 2009.
- Jones, A. E., Anderson, P. S., Wolff, E. W., Roscoe, H. K., Marshall, G. J., Richter, A., Brough, N., and Colwell, S. R.: Vertical structure of Antarctic tropospheric ozone depletion events: characteristics and broader implications, *Atmos. Chem. Phys.*, 10, 7775–7794, doi:10.5194/acp-10-7775-2010, 2010.
- 25 Koo, J.-H., Wang, Y., Kurosu, T. P., Chance, K., Rozanov, A., Richter, A., Oltmans, S. J., Thompson, A. M., Hair, J. W., Fenn, M. A., Weinheimer, A. J., Ryerson, T. B., Solberg, S., Huey, L. G., Liao, J., Dibb, J. E., Neuman, J. A., Nowak, J. B., Pierce, R. B., Natarajan, M., and Al-Saadi, J.: Characteristics of tropospheric ozone depletion events in the Arctic spring: analysis of the ARC-TAS, ARCPAC, and ARCIONS measurements and satellite BrO observations, *Atmos. Chem. Phys.*, 12, 9909–9922, doi:10.5194/acp-12-9909-2012, 2012.
- 30

- Krnavek, L., Simpson, W. R., Carlson, D., Domine, F., Douglas, T. A., and Sturm, M.: The chemical composition of surface snow in the Arctic: examining marine, terrestrial, and atmospheric influences, *Atmos. Environ.*, 50, 349–359, doi:10.1016/j.atmosenv.2011.11.033, 2012.
- Lehrer, E., Hönninger, G., and Platt, U.: A one dimensional model study of the mechanism of halogen liberation and vertical transport in the polar troposphere, *Atmos. Chem. Phys.*, 4, 2427–2440, doi:10.5194/acp-4-2427-2004, 2004.
- Liao, J., Sihler, H., Huey, L. G., Neuman, J. A., Tanner, D. J., Friess, U., Platt, U., Flocke, F. M., Orlando, J. J., Shepson, P. B., Beine, H. J., Weinheimer, A. J., Sjostedt, S. J., Nowak, J. B., Knapp, D. J., Staebler, R. M., Zheng, W., Sander, R., Hall, S. R., and Ullmann, K.: A comparison of Arctic BrO measurements by chemical ionization mass spectrometry and long path-differential optical absorption spectroscopy, *J. Geophys. Res.*, 116, 1–14, doi:10.1029/2010JD014788, 2011.
- Liao, J., Huey, L. G., Tanner, D. J., Flocke, F. M., Orlando, J. J., Neuman, J. A., Nowak, J. B., Weinheimer, A. J., Hall, S. R., Smith, J. N., Fried, A., Staebler, R. M., Wang, Y., Koo, J.-H., Cantrell, C. A., Weibring, P., Walega, J., Knapp, D. J., Shepson, P. B., and Stephens, C. R.: Observations of inorganic bromine (HOBr, BrO, and Br₂) speciation at Barrow, Alaska, in spring 2009, *J. Geophys. Res.*, 117, D00R16, doi:10.1029/2011JD016641, 2012.
- Liao, J., Huey, L. G., Liu, Z., Tanner, D. J., Cantrell, C. A., Orlando, J. J., Flocke, F. M., Shepson, P. B., Weinheimer, A. J., Hall, S. R., Ullmann, K., Beine, H. J., Wang, Y., Ingall, E. D., Stephens, C. R., Hornbrook, R. S., Apel, E. C., Riemer, D., Fried, A., Mauldin III, R. L., Smith, J. N., Staebler, R. M., Neuman, J. A., and Nowak, J. B.: High levels of molecular chlorine in the Arctic atmosphere, *Nat. Geosci.*, 7, 91–94, doi:10.1038/ngeo2046, 2014.
- Malicet, J., Daumont, D., Charbonnier, J., Parisse, C., Chakir, A., and Brion, J.: Ozone UV spectroscopy. II. Absorption cross-sections and temperature dependence, *J. Atmos. Chem.*, 21, 263–273, doi:10.1007/BF00696758, 1995.
- McConnell, J. C., Henderson, G. S., Barrie, L., Bottenheim, J., Niki, H., Langford, C. H., and Templeton, E. M. J.: Photochemical bromine production implicated in Arctic boundary-layer ozone depletion, *Nature*, 355, 150–152, doi:10.1038/355150a0, 1992.
- McElroy, C. T., McLinden, C. A., and McConnell, J. C.: Evidence for bromine monoxide in the free troposphere during the arctic polar sunrise, *Nature*, 397, 338–341, 1999.
- Moore, C. W., Obrist, D., Steffen, A., Staebler, R. M., Douglas, T. A., Richter, A., and Nghiem, S. V.: Convective forcing of mercury and ozone in the Arctic boundary layer induced by leads in sea ice., *Nature*, 506, 81–84, doi:10.1038/nature12924, 2014.

- Mozurkewich, M.: Mechanisms for the release of halogens from sea-salt particles by free radical reactions, *J. Geophys. Res.*, 100, 14199–14207, 1995.
- Neuman, J. A., Nowak, J. B., Huey, L. G., Burkholder, J. B., Dibb, J. E., Holloway, J. S., Liao, J., Peischl, J., Roberts, J. M., Ryerson, T. B., Scheuer, E., Stark, H., Stickel, R. E., Tanner, D. J., and Weinheimer, A.: Bromine measurements in ozone depleted air over the Arctic Ocean, *Atmos. Chem. Phys.*, 10, 6503–6514, doi:10.5194/acp-10-6503-2010, 2010.
- Nghiem, S. V., Clemente-Colón, P., Douglas, T., Moore, C., Obrist, D., Perovich, D. K., Pratt, K. A., Rigor, I. G., Simpson, W., Shepson, P. B., Steffen, A., and Woods, J.: Studying bromine, ozone, and mercury chemistry in the Arctic, *EOS T. Am. Geophys. Un.*, 94, 289–291, doi:10.1002/2013EO330002, 2013.
- Oltmans, S. J., Johnson, B. J., and Harris, J. M.: Springtime boundary layer ozone depletion at Barrow, Alaska: meteorological influence, year-to-year variation, and long-term change, *J. Geophys. Res.*, 117, D00R18, doi:10.1029/2011JD016889, 2012.
- Parrella, J. P., Jacob, D. J., Liang, Q., Zhang, Y., Mickley, L. J., Miller, B., Evans, M. J., Yang, X., Pyle, J. A., Theys, N., and Van Roozendael, M.: Tropospheric bromine chemistry: implications for present and pre-industrial ozone and mercury, *Atmos. Chem. Phys.*, 12, 6723–6740, doi:10.5194/acp-12-6723-2012, 2012.
- Payne, V. H., Clough, S. A., Shephard, M. W., Nassar, R., and Logan, J. A.: Information-centered representation of retrievals with limited degrees of freedom for signal: application to methane from the tropospheric emission spectrometer, *J. Geophys. Res.*, 114, D10307, doi:10.1029/2008JD010155, 2009.
- Piot, M. and von Glasow, R.: The potential importance of frost flowers, recycling on snow, and open leads for ozone depletion events, *Atmos. Chem. Phys.*, 8, 2437–2467, doi:10.5194/acp-8-2437-2008, 2008.
- Platt, U., and Hönninger, G.: The role of halogen species in the troposphere, *Chemosphere*, 52, 325–338, doi:10.1016/S0045-6535(03)00216-9, 2003.
- Pöhler, D., Vogel, L., Friess, U., and Platt, U.: Observation of halogen species in the Amundsen Gulf, Arctic, by active long-path differential optical absorption spectroscopy, *P. Natl. Acad. Sci. USA*, 107, 6582–6587, doi:10.1073/pnas.0912231107, 2010.
- Pratt, K. A., Custard, K. D., Shepson, P. B., Douglas, T. A., Pöhler, D., General, S., Zielcke, J., Simpson, W. R., Platt, U., Tanner, D. J., Gregory Huey, L., Carlsen, M., and Stirm, B. H.: Photochemical production of molecular bromine in Arctic surface snowpacks, *Nat. Geosci.*, 6, 351–356, doi:10.1038/ngeo1779, 2013.

- Richter, A., Wittrock, F., Eisinger, M., and Burrows, J. P.: GOME observations of tropospheric BrO in Northern Hemispheric spring and summer 1997, *Geophys. Res. Lett.*, 25, 2683–2686, 1998.
- Rodgers, C. D.: *Inverse Methods For Atmospheric Sounding: Theory and Practice*, World Scientific, Singapore, 2000.
- 5 Rozanov, A., Bovensmann, H., Bracher, A., Hrechanyy, S., Rozanov, V., Sinnhuber, M., Stroh, F., and Burrows, J.: NO₂ and BrO vertical profile retrieval from SCIAMACHY limb measurements: sensitivity studies, *Adv. Space Res.*, 36, 846–854, doi:10.1016/j.asr.2005.03.013, 2005.
- Saiz-Lopez, A. and von Glasow, R.: Reactive halogen chemistry in the troposphere, *Chem. Soc. Rev.*, 41, 6448–6472, 2012.
- 10 Salawitch, R. J., Canty, T., Kurosu, T., Chance, K., Liang, Q., da Silva, A., Pawson, S., Nielsen, J. E., Rodriguez, J. M., Bhartia, P. K., Liu, X., Huey, L. G., Liao, J., Stickel, R. E., Tanner, D. J., Dibb, J. E., Simpson, W. R., Donohoue, D., Weinheimer, A., Flocke, F., Knapp, D., Montzka, D., Neuman, J. A., Nowak, J. B., Ryerson, T. B., Oltmans, S., Blake, D. R., Atlas, E. L., Kinnison, D. E., Tilmes, S., Pan, L. L., Hendrick, F., Van Roozendaal, M., Kreher, K., Johnston, P. V., Gao, R. S., Johnson, B.,
- 15 Bui, T. P., Chen, G., Pierce, R. B., Crawford, J. H., and Jacob, D. J.: A new interpretation of total column BrO during Arctic spring, *Geophys. Res. Lett.*, 37, L21805, doi:10.1029/2010GL043798, 2010.
- Schroeder, W., Anlauf, K., Barrie, L., and Lu, J.: Arctic springtime depletion of mercury, *Nature*, 16–17, 394, doi:10.1038/28530, 1998.
- 20 Sihler, H., Platt, U., Beirle, S., Marbach, T., Kühl, S., Dörner, S., Verschaeve, J., Frieß, U., Pöhler, D., Vogel, L., Sander, R., and Wagner, T.: Tropospheric BrO column densities in the Arctic derived from satellite: retrieval and comparison to ground-based measurements, *Atmos. Meas. Tech.*, 5, 2779–2807, doi:10.5194/amt-5-2779-2012, 2012.
- Simpson, W. R., Carlson, D., Hönninger, G., Douglas, T. A., Sturm, M., Perovich, D., and Platt, U.: First-year sea-ice contact predicts bromine monoxide (BrO) levels at Barrow, Alaska better than potential frost flower contact, *Atmos. Chem. Phys.*, 7, 621–627, doi:10.5194/acp-7-621-2007, 2007a.
- 25 Simpson, W. R., von Glasow, R., Riedel, K., Anderson, P., Ariya, P., Bottenheim, J., Burrows, J., Carpenter, L. J., Frieß, U., Goodsite, M. E., Heard, D., Hutterli, M., Jacobi, H.-W., Kaleschke, L., Neff, B., Plane, J., Platt, U., Richter, A., Roscoe, H., Sander, R., Shepson, P., Sodeau, J., Steffen, A., Wagner, T., and Wolff, E.: Halogens and their role in polar boundary-layer ozone depletion, *Atmos. Chem. Phys.*, 7, 4375–4418, doi:10.5194/acp-7-4375-2007, 2007b.
- 30

- Spicer, C. W., Plastridge, R. A., Foster, K. L., Finlayson-Pitts, B. J., Bottenheim, J. W., Grannas, A. M., and Shepson, P. B.: Molecular halogens before and during ozone depletion events in the Arctic at polar sunrise: concentrations and sources, *Atmos. Environ.*, 36, 2721–2731, doi:10.1016/S1352-2310(02)00125-5, 2002.
- 5 Steffen, A., Douglas, T., Amyot, M., Ariya, P., Aspmo, K., Berg, T., Bottenheim, J., Brooks, S., Cobbett, F., Dastoor, A., Dommergue, A., Ebinghaus, R., Ferrari, C., Gardfeldt, K., Goodsite, M. E., Lean, D., Poulain, A. J., Scherz, C., Skov, H., Sommar, J., and Temme, C.: A synthesis of atmospheric mercury depletion event chemistry in the atmosphere and snow, *Atmos. Chem. Phys.*, 8, 1445–1482, doi:10.5194/acp-8-1445-2008, 2008.
- 10 Sturm, M. and Stuefer, S.: Wind-blown flux rates derived from drifts at arctic snow fences, *J. Glaciol.*, 59, 21–34, doi:10.3189/2013JoG12J110, 2013.
- [Stutz, J., Thomas, J. L., Hurlock, S. C., Schneider, M., von Glasow, R., Piot, M., Gorham, K., Burkhardt, J. F., Ziemba, L., Dibb, J. E., and Lefer, B. L.: Longpath DOAS observations of surface BrO at Summit, Greenland, *Atmospheric Chemistry and Physics*, 11, 9899–9910, doi:10.5194/acp-11-9899-2011, 2011.](#)
- 15 Tackett, P. J., Cavender, A. E., Keil, A. D., Shepson, P. B., Bottenheim, J. W., Morin, S., Deary, J., Steffen, A., and Doerge, C.: A study of the vertical scale of halogen chemistry in the Arctic troposphere during Polar Sunrise at Barrow, Alaska, *J. Geophys. Res.*, 112, D07306, doi:10.1029/2006JD007785, 2007.
- 20 Tarasick, D. W. and Bottenheim, J. W.: Surface ozone depletion episodes in the Arctic and Antarctic from historical ozonesonde records, *Atmos. Chem. Phys.*, 2, 197–205, doi:10.5194/acp-2-197-2002, 2002.
- Theys, N., Van Roozendaal, M., Errera, Q., Hendrick, F., Daerden, F., Chabrillat, S., Dorf, M., Pfeilsticker, K., Rozanov, A., Lotz, W., Burrows, J. P., Lambert, J.-C., Goutail, F., Roscoe, H. K., and De Mazière, M.: A global stratospheric bromine monoxide climatology based on the BASCOE chemical transport model, *Atmos. Chem. Phys.*, 9, 831–848, doi:10.5194/acp-9-831-2009, 2009.
- 25 Theys, N., Van Roozendaal, M., Hendrick, F., Yang, X., De Smedt, I., Richter, A., Begoin, M., Errera, Q., Johnston, P. V., Kreher, K., and De Mazière, M.: Global observations of tropospheric BrO columns using GOME-2 satellite data, *Atmos. Chem. Phys.*, 11, 1791–1811, doi:10.5194/acp-11-1791-2011, 2011.
- 30 Toom-Saunry, D. and Barrie, L. A.: Chemical composition of snowfall in the high Arctic: 1990–1994, *Atmos. Environ.*, 36, 2683–2693, 2002.

- Toyota, K., McConnell, J. C., Staebler, R. M., and Dastoor, A. P.: Air–snowpack exchange of bromine, ozone and mercury in the springtime Arctic simulated by the 1-D model PHANTAS – Part 1: In-snow bromine activation and its impact on ozone, *Atmos. Chem. Phys.*, 14, 4101–4133, doi:10.5194/acp-14-4101-2014, 2014.
- 5 Tuckermann, M., R., A., Golz, C., Lorenzen-Schmidt, H., Senne, T., Stutz, J., Trost, B., Unold, W., and Platt, U.: DOAS-observation of halogen radical-catalysed arctic boundary layer ozone destruction during the ARCTOC-campaigns 1995 and 1996 in Ny-Alesund, Spitsbergen, *Tellus B*, 49, 533–555, doi:10.1034/j.1600-0889.49.issue5.9.x, 1997.
- 10 Vandaele, A., Hermans, C., Simon, P., Carleer, M., Colin, R., Fally, S., Mérienne, M., Jenouvrier, A., and Coquart, B.: Measurements of the NO₂ absorption cross-section from 42 000 cm⁻¹ to 10 000 cm⁻¹ (238–1000 nm) at 220 K and 294 K, *J. Quant. Spectrosc. Ra.*, 59, 171–184, doi:10.1016/S0022-4073(97)00168-4, 1998.
- von Clarmann, T. and Grabowski, U.: Elimination of hidden a priori information from remotely sensed profile data, *Atmos. Chem. Phys.*, 7, 397–408, doi:10.5194/acp-7-397-2007, 2007.
- 15 Wagner, T. and Platt, U.: Satellite mapping of enhanced BrO concentrations in the troposphere, *Nature*, 395, 486–490, 1998.
- Wilmouth, D. M., Hanisco, T. F., Donahue, N. M., and Anderson, J. G.: Fourier transform ultraviolet spectroscopy of the $A^2\Pi_{3/2} \leftarrow X^2\Pi_{3/2}$ transition of BrO, *J. Phys. Chem. A*, 103, 8935–8945, doi:10.1021/jp991651o, 1999.
- 20 Wren, S. N., Donaldson, D. J., and Abbatt, J. P. D.: Photochemical chlorine and bromine activation from artificial saline snow, *Atmos. Chem. Phys.*, 13, 9789–9800, doi:10.5194/acp-13-9789-2013, 2013.
- Yang, X., Pyle, J. A., Cox, R. A., Theys, N., and Van Roozendael, M.: Snow-sourced bromine and its implications for polar tropospheric ozone, *Atmos. Chem. Phys.*, 10, 7763–7773, doi:10.5194/acp-10-7763-2010, 2010.
- 25

Table 1. Absorber cross sections used in the MAX-DOAS fitting.

Species	Cross Section
BrO (223 K)	Wilmouth et al. (1999)
O ₃ (243 K)	Malicet et al. (1995)
NO ₂ (220 K)	Vandaele et al. (1998)
O ₄	Hermans et al. (2001)
Ring	Determined from zenith spectra using Chance and Spurr (1997)

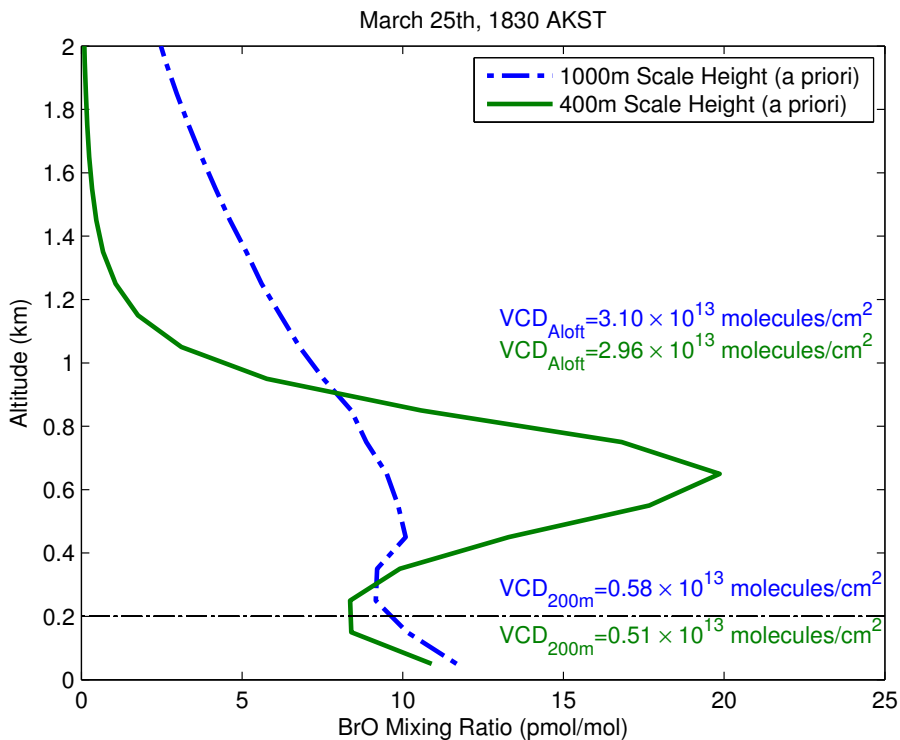


Figure 1. A sample profile retrieval of BrO at the BARC building. The blue line represents the profile retrieved using an a priori profile that exponentially decays with a scale height of 1000 m, while the green represents quantities retrieved using an a priori profile that exponentially decays with a scale height of 400 m (a priori used for this study). The dashed lines indicate layer boundaries determined from the ensemble of retrievals over the course of this study. The partial VCD values noted on the figure correspond to layer selections used in this study. The VCD_{200m} is the integral of the retrieved profile from 0–200 m and the VCD_{Aloft} is integrated from 200 to 2000 m.

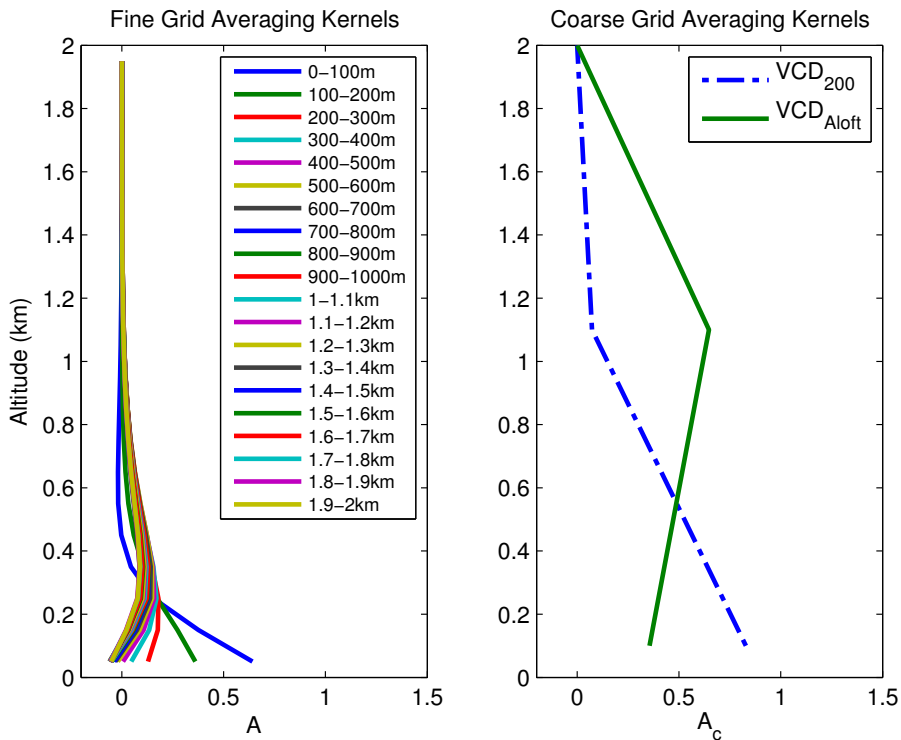


Figure 2. An illustration of the grid coarsening of the BrO averaging kernels. These averaging kernels correspond to the retrieval shown in green on Fig. 1. Averaging kernels for the original retrieval (left) and for the coarse grid (right).

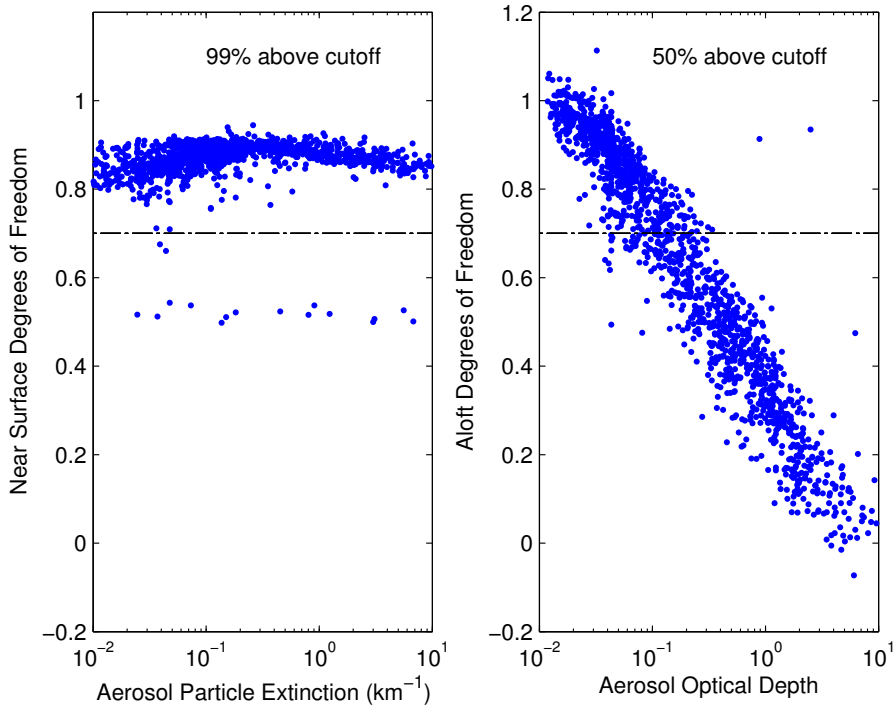


Figure 3. The left panel shows the degrees of freedom associated with the $\text{VCD}_{200\text{m}}$ as a function of near-surface aerosol particle extinction. The right panel shows the degrees of freedom associated with the $\text{VCD}_{\text{Residual}}$ as a function of the aerosol optical depth. The dashed line illustrates the cutoff we have chosen for sufficient information content.

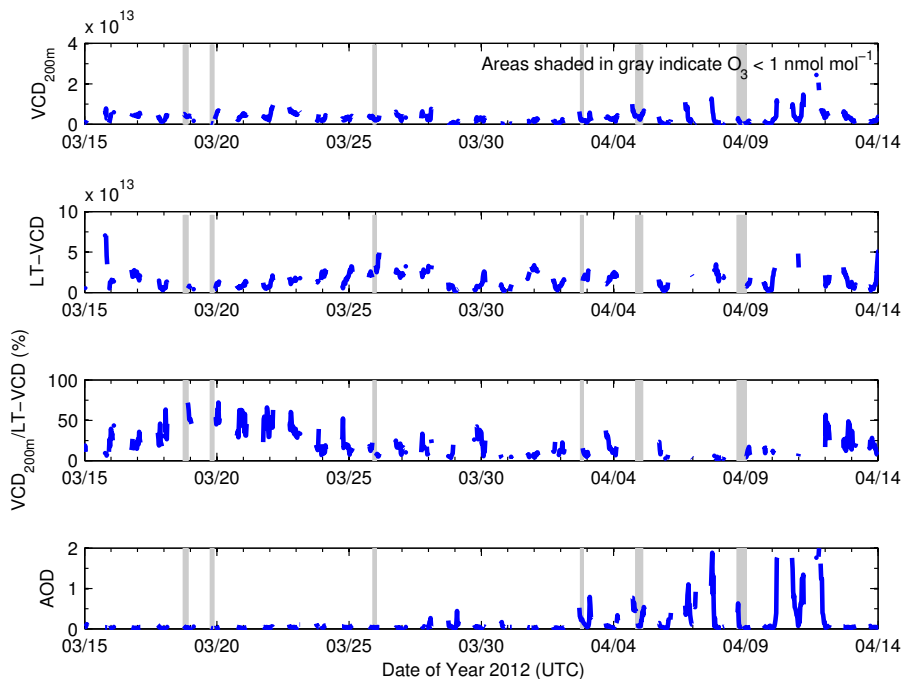


Figure 4. A portion of the timeseries of BrO observed during this study. The top panel represents the VCD_{200m} , the second panel represents the $LT-VCD$, both of which have units of molecules cm^{-2} . The third panel shows the percentage of the $LT-VCD$ observed in the lowest 200 m, while the bottom panel shows the aerosol optical depth over the course of this study. In the third panel, ratios are not calculated for events that have a $LT-VCD$ below 5×10^{12} molecules cm^{-2} . Shaded areas represent potentially titrated air masses near the surface ($O_3 < 1 \text{ nmol mol}^{-1}$). The full timeseries can be found in the Supplement.

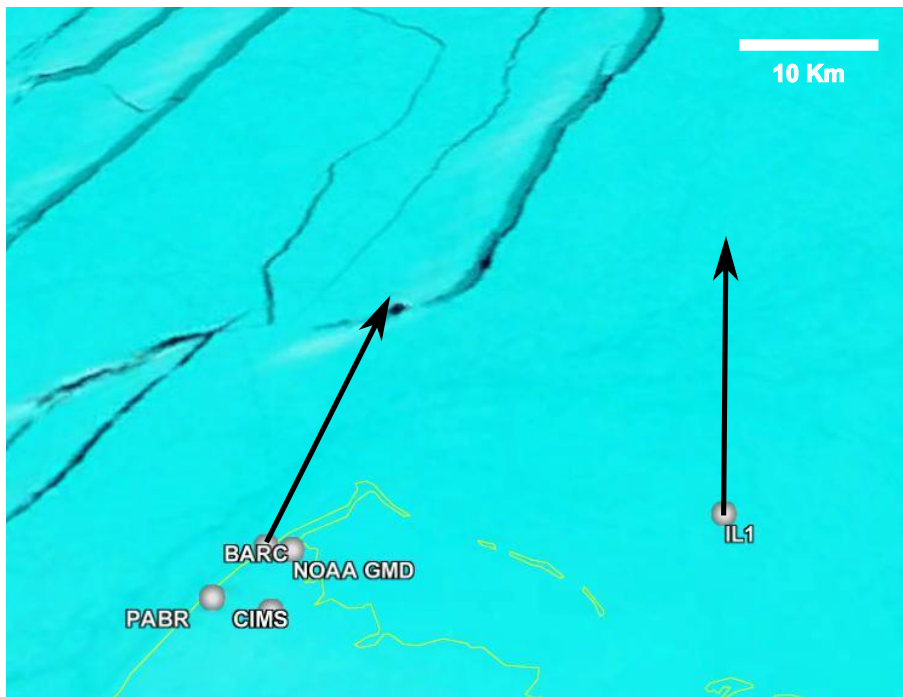


Figure 5. Field locations during the BROMEX field campaign overlain on [Moderate Resolution Imaging Spectrometer data from the Environmental Systems Research Institute Aqua satellite \(ESR17.2.1_bands\) world image](#). This ice cover image is from March 13th, 2012. These locations are Barrow Arctic Research Center (BARC), Chemical Ionization Mass Spectrometry (CIMS), NOAA Global Monitoring Division (NOAA GMD) station, IceLander 1 (IL1) buoy, and Barrow Airport (PABR), nearby where most of Barrow's population resides. The distance between BARC and IL1 is about 36 km. [Viewing azimuths for each DOAS instrument are indicated with black arrows.](#)

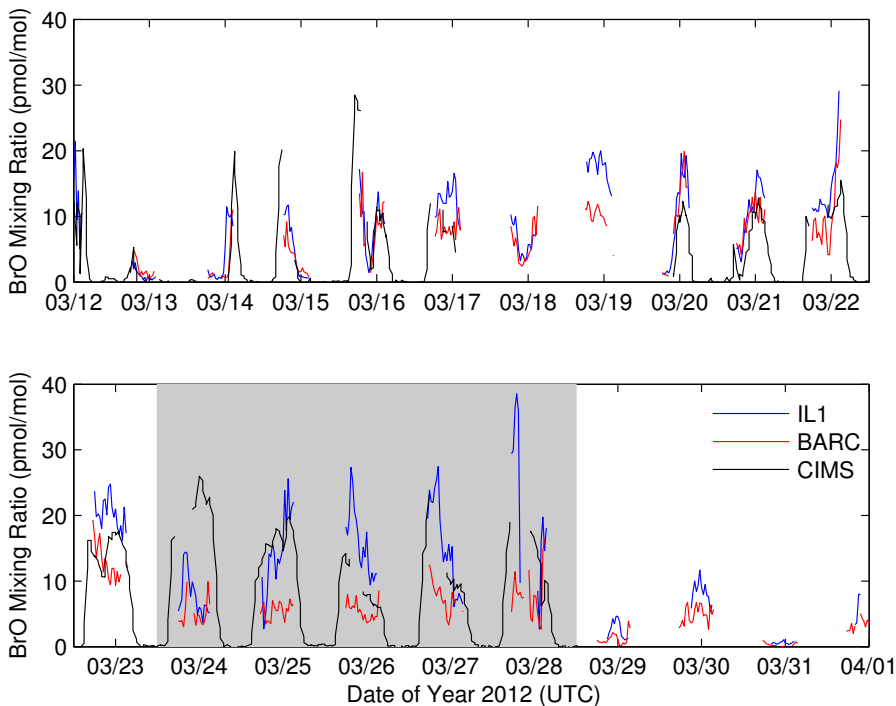


Figure 6. A timeseries of 30 min averaged BrO measured using CIMS, compared with average BrO in the lowest 100 m measured by MAX-DOAS at two different sites. The grey area indicates times when there were significant differences in BrO observed between MAX-DOAS sites at the BARC Building and on land fast ice 36 km NE of the BARC building (IL1).

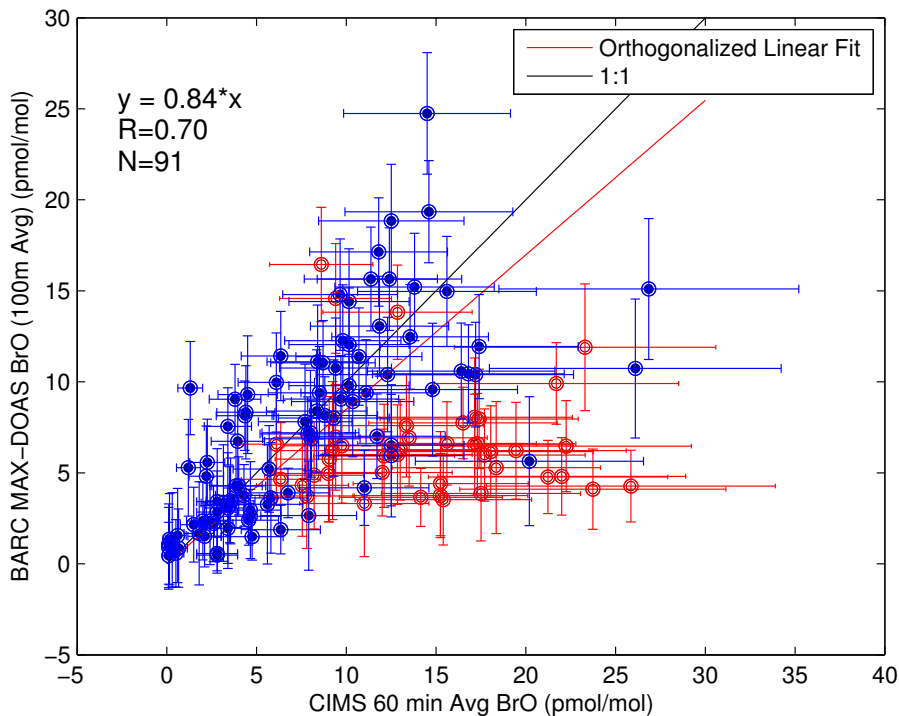


Figure 7. The correlation of 60 min averaged CIMS BrO with BrO retrieved in the lowest 100 m using MAX-DOAS. Red circles indicate times when we observed a chemical gradient between field sites, which are excluded from this correlation.

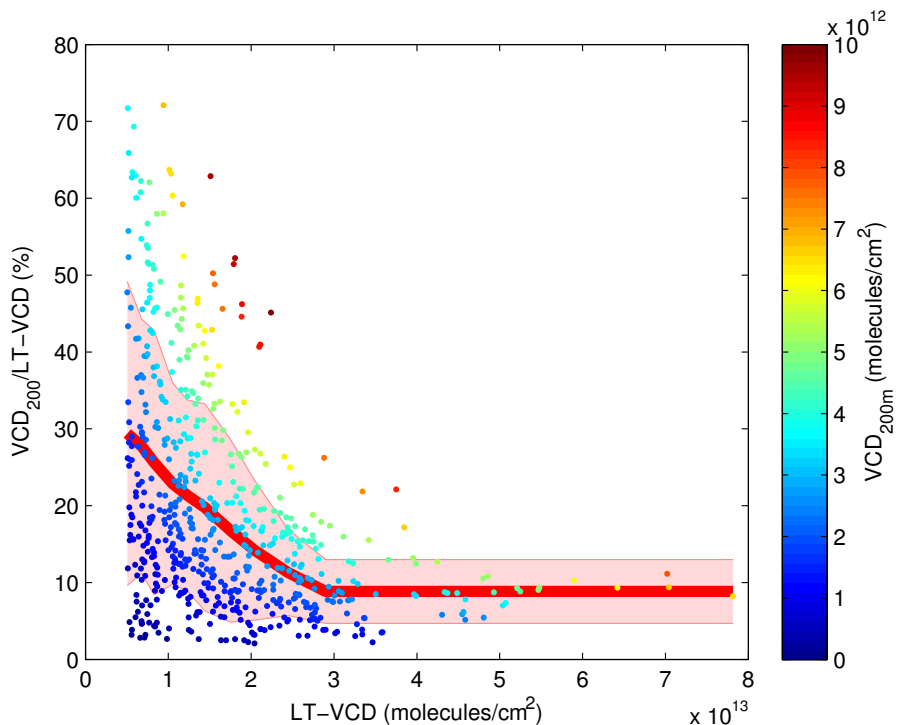


Figure 8. The relationship between the total BrO activation, as measured by the LT-VCD, and the vertical structure of the activation event. The red line represents the mean percentage of BrO in the lowest 200 m as a function of the LT-VCD, calculated from deciles on the x axis, while the shaded region represents one standard deviation. The coloration indicates the VCD_{200m} . In this plot LT-VCD values below 5×10^{12} molecules cm^{-2} are eliminated to avoid calculating percentages from near zero amounts of BrO.

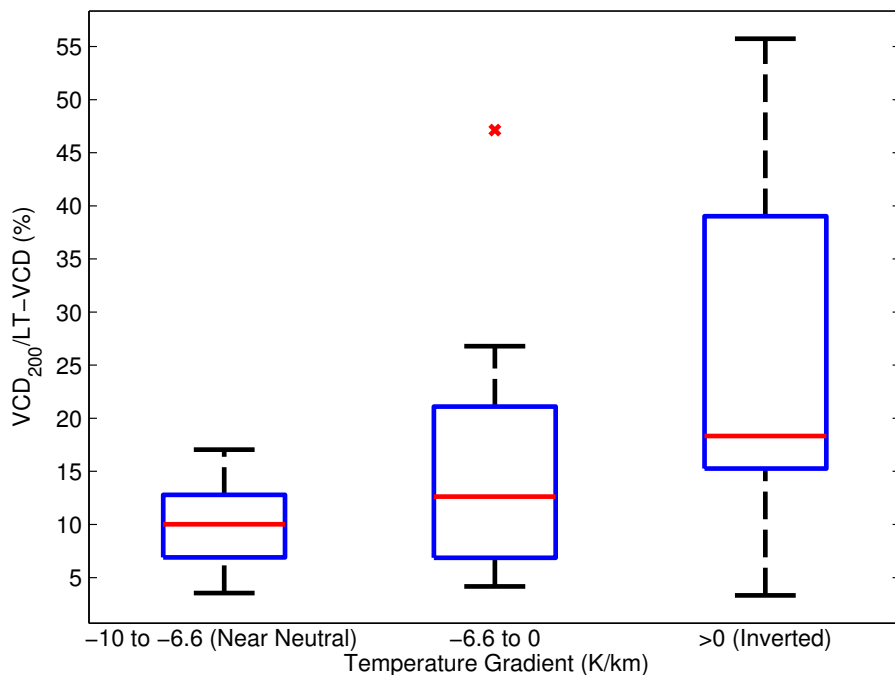


Figure 9. The relationship between daily estimated temperature gradients vs. the average percentage of BrO observed in the near surface layer during that day is shown here using a box and whisker plot. The data are split such that each bin comprises ≈ 20 days worth of data. The red lines show the median value for each bin, while the blue box encloses the 25–75th percentile and the whiskers show the full range of data excluding outliers (\times). Outliers are points that are outside 3σ for the corresponding group.

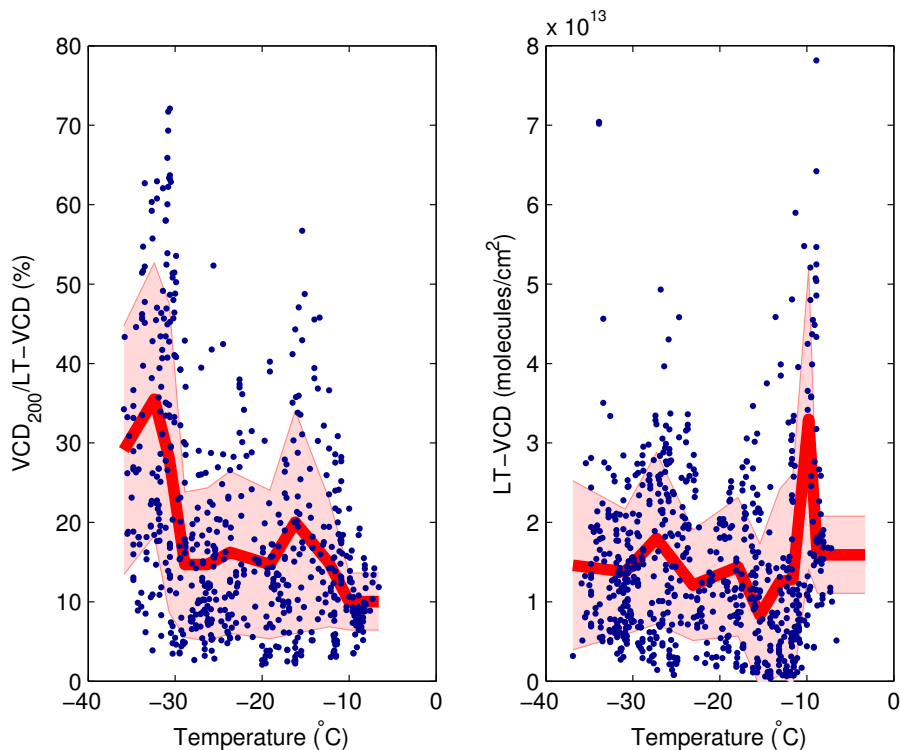


Figure 10. The relationship between BrO and temperature. The left panel shows the percentage of BrO in the lowest 200 m vs. the near-surface temperature, while the right panel shows the LT-VCD vs. the near-surface temperature. The red line represents the mean, calculated from deciles on the x axis, while the shaded region represents one standard deviation. In the left panel, LT-VCD values below 5×10^{12} molecules cm^{-2} are eliminated to avoid calculating percentages from near zero amounts of BrO.

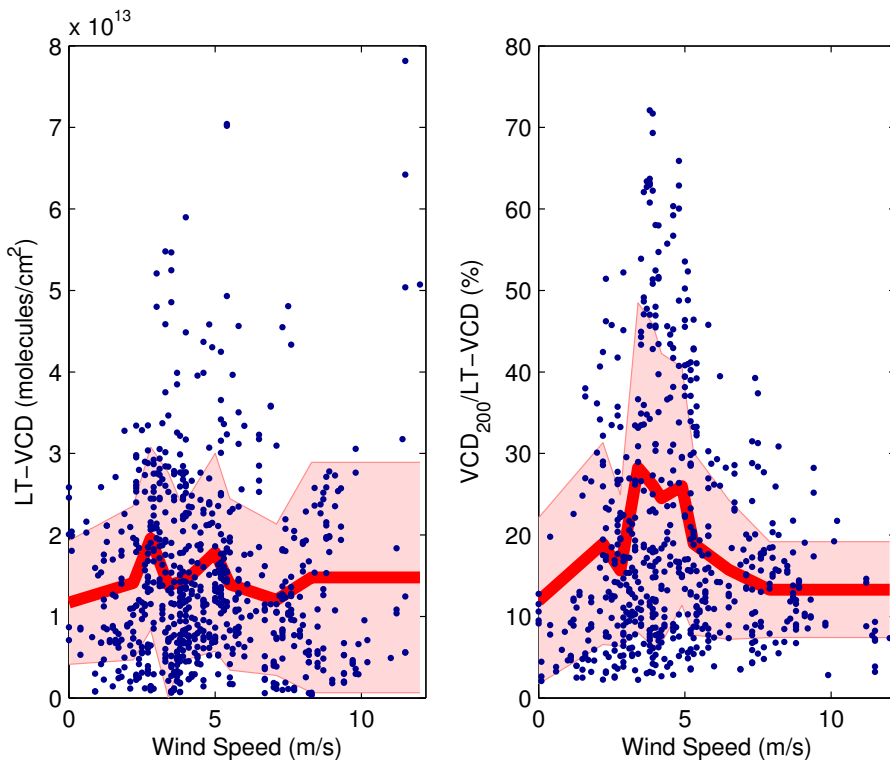


Figure 11. The left panel shows the relationship between the BrO LT-VCD and wind speed, while the right panel shows percentage of BrO in the lowest 200 m vs. the wind speed. In both cases, the red line represents the mean as a function of wind speed, calculated from deciles on the x axis, while the shaded region represents one standard deviation.

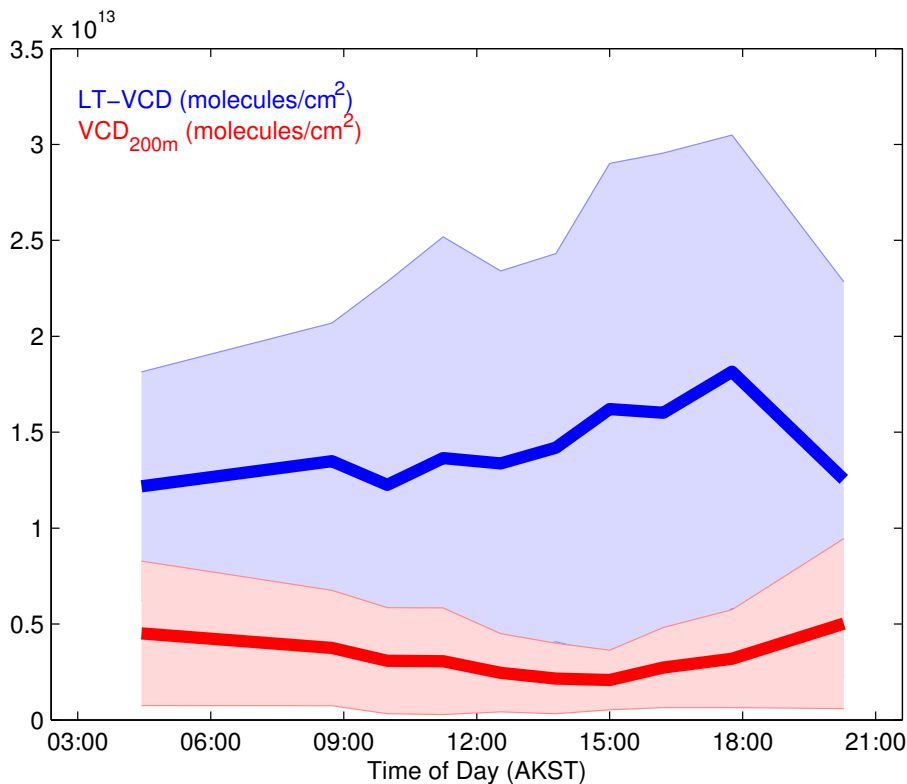


Figure 12. The diurnal cycling of the BrO LT-VCD (blue) and VCD_{200m} (red). The solid lines represent the mean VCD as a function of time of day, while the shaded region represents one standard deviation. The shaded regions are ~~symetric~~ symmetric about the mean in both cases, however the cycling of the VCD_{200m} is overlain on the cycling of the LT-VCD, partially obscuring the standard deviation of the LT-VCD.

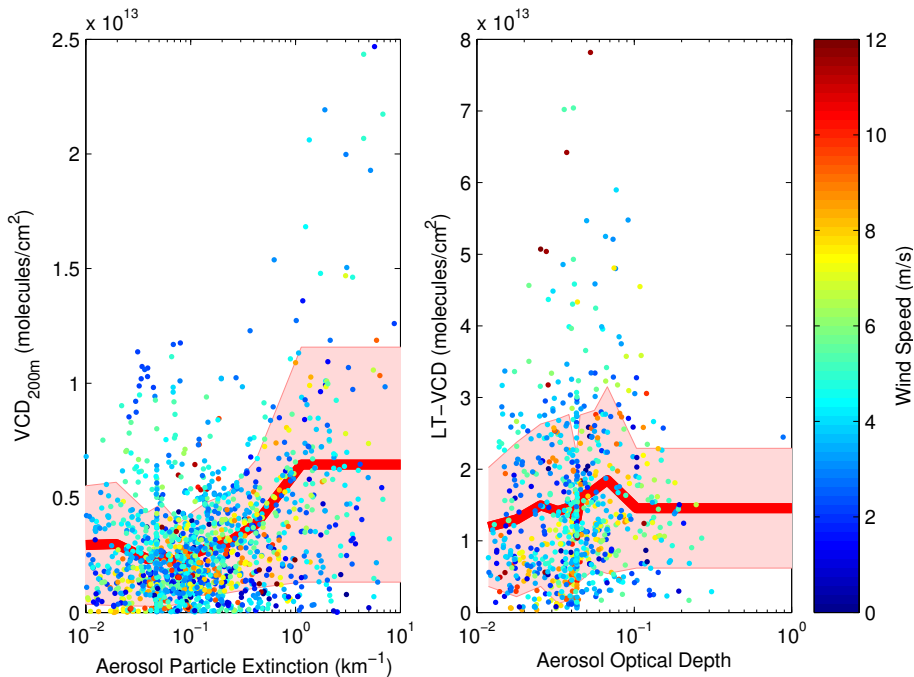


Figure 13. The left panel shows the relationship between the BrO VCD_{200m} and the near-surface aerosol particle extinction. The right panel shows the relationship between the BrO LT-VCD and the aerosol optical depth. In both plots the x axis is a log scale. The red line represents the mean VCD, calculated from deciles on the x axis, while the shaded region represents one standard deviation. In both cases, the coloration indicates the wind speed.